

Palaeomagnetic and geochronological evidence for a major middle Miocene unconformity in Söke Basin (western Anatolia) and its tectonic implications for the Aegean region

Bora Uzel^{1*}, Ökmen Sümer¹, Murat Özkaptan², Çağlar Özkaymak³, Klaudia Kuiper⁴, Hasan Sözbilir¹, Nuretdin Kaymakci⁵, Uğur İnci¹ & Cornelis G. Langereis⁶

¹ Department of Geological Engineering, Dokuz Eylül University, İzmir TR-35160, Turkey


² Karadeniz Technical University, Department of Geophysical Engineering, TR-61080 Trabzon, Turkey

³ Department of Geological Engineering, Afyon Kocatepe University, Afyon TR-03200, Turkey

⁴ Department of Earth and Life Sciences, Vrije Universiteit, Amsterdam 1081-HV, Netherlands

⁵ Department of Geological Engineering, Middle East Technical University, Ankara TR-06531, Turkey

⁶ Fort Hoofddijk Paleomagnetic Laboratory, Utrecht University, Utrecht 3584-CD, Netherlands

 B.U., 0000-0003-1703-5026; K.K., 0000-0001-6345-5019; N.K., 0000-0002-7618-0226; C.G.L., 0000-0001-9232-2178

* Correspondence: bora.uzel@deu.edu.tr

Abstract: Cenozoic convergence between the Eurasian and African plates and concurrent slab roll-back processes have produced a progressive extension in back-arc areas, such as the Aegean region and western Anatolia. There is still a long-standing controversy as to whether this was a continuous or stepwise process. To shed light on this controversy and on the driving mechanism of regional extension, we present palaeomagnetic and geochronological results from the Söke Basin located at the southeastern rim of the İzmir–Balıkesir Transfer Zone. Our improved geochronology shows that volcanic activity in the region occurred between 11.66 and 12.85 Ma. Middle to late Miocene palaeomagnetic data for the Söke Basin show a *c.* 23° clockwise rotation, whereas early Miocene data show a *c.* 28° counterclockwise rotation. The primary nature of the magnetization is indicated by a positive tilt test. The resulting *c.* 51° counterclockwise rotations during the middle Miocene signify a major tectonic reorganization, during a period when an interruption of exhumation of metamorphic massifs has been reported. We suggest that the İzmir–Balıkesir Transfer Zone is the main driver of the reorganization in the region. The regional fingerprint of this tectonic reorganization coincides with the acceleration of trench retreat and illustrates the surface impact of tearing of the Hellenic slab.

Supplementary material: Details of ⁴⁰Ar/³⁹Ar analysis including heating steps and the output (.pmag) file including details of paleomagnetic analysis performed in this study are available at <https://doi.org/10.6084/m9.figshare.c.3690871>

Received 12 January 2016; **revised** 6 December 2016; **accepted** 3 January 2017

The Cenozoic tectonic evolution of the Aegean region has been largely shaped by the development of a number of detachment systems that resulted from collision between the Eurasian plate and the African and Arabian plates (Fig. 1a). Lying on the overriding plate, the Aegean region is mainly dominated by NNE extension since the late Eocene (Gautier *et al.* 1999; Forster & Lister 2009; Tirel *et al.* 2009; Jolivet & Brun 2010; van Hinsbergen & Schmidt 2012). Many studies hold the slab edge processes related to the northward subducting African slab below Eurasia responsible for regional extension in western Anatolia (Le Pichon & Angelier 1979; Meulenkamp *et al.* 1988; van Hinsbergen *et al.* 2005a; van Hinsbergen *et al.* 2010b; Biryol *et al.* 2011), although others indicate the westward escape of Anatolia (Şengör 1979; Şengör & Yılmaz 1981; Şengör *et al.* 1985; Dewey *et al.* 1986). Irrespective of its cause, extension in the region is compensated by large-scale extensional detachments and associated high-angle normal faults, along which a series of core complexes and gneissic domes are exhumed. It seems that each core complex accommodated a different amount of extension. Hence, the lateral variation of extension is compensated by the development of transfer zones, such as the İzmir–Balıkesir Transfer Zone and the Mid-Cycladic Lineament (Morris & Anderson 1996; Walcott & White 1998; Ring *et al.* 1999; Pe-Piper *et al.* 2002; Sözbilir *et al.* 2003; Philippon *et al.* 2012, 2014; Uzel *et al.* 2015). Recent studies have demonstrated that the İzmir–Balıkesir Transfer Zone is a lithospheric-scale structural element that accommodated differential displacement

between the Cycladic and Menderes core complexes (Sözbilir *et al.* 2011; Gessner *et al.* 2013; Uzel *et al.* 2013) and led to complex rotational deformation documented by, for example, Kondopoulou *et al.* (2011) and Uzel *et al.* (2015).

A key controversy on core complex evolution in western Anatolia is whether extension and/or basin formation evolved continuously or episodically. One group argues for a continuous evolution (e.g. Seyitoğlu *et al.* 2000, 2002, 2004; Glodny & Hetzel 2007), whereas another group of researchers share the view that deformation is episodic and extension phases are separated by contraction phase(s) and/or tectonic quiescence(s) (e.g. Koçyiğit *et al.* 1999; Yılmaz *et al.* 2000; Bozkurt 2001a,b; Sözbilir 2001; Bozkurt & Sözbilir 2004, 2006; Kaya *et al.* 2004, 2007; Purvis & Robertson 2004, 2005a; Beccaletto & Steiner 2005; Bozkurt & Mittweide 2005; Koçyiğit 2005;

Kaymakci 2006; Emre & Sözbilir 2007; Koçyiğit & Deveci 2007). Distinguishing these possibilities is made difficult because it is hard to identify in the field whether a family of structures belongs to the same tectonic episode or developed in different tectonic episodes (Uzel *et al.* 2013). Therefore, many age data from metamorphic and tectonic structures have been obtained to try and understand the exhumation pattern of core complexes and to identify the tectonic phases (Gessner *et al.* 2001, 2013; Ring *et al.* 2003; Thomson & Ring 2006; Bozkurt *et al.* 2011; Hetzel *et al.* 2013; Brun *et al.* 2016). Simultaneously, palaeomagnetic studies on the Anatolian plate were carried out but were generally concerned

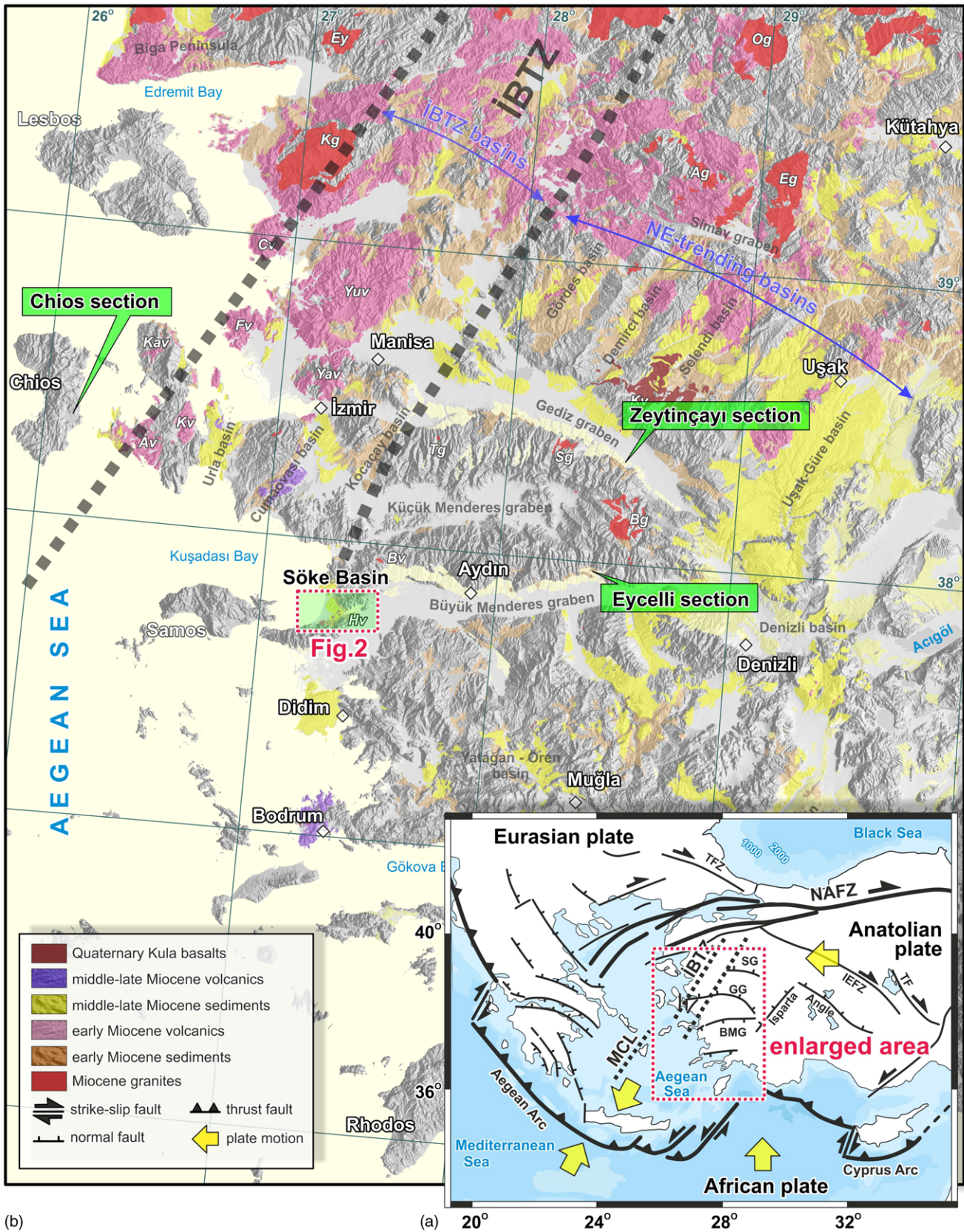


Fig. 1. (a) Simplified map showing the major (plate) tectonic elements and configuration of the Aegean region (Koçyiğit & Özaçar 2003; Kaymakci *et al.* 2007; and our observations). NAFZ, North Anatolian Fault Zone; TF, Tuz Gölü Fault; IEFZ, İnönü-Eskişehir Fault Zone; BMG, Büyük Menderes Graben; GG, Gediz Graben; SG, Simav Graben; TFZ, Thrace Fault Zone; İBTZ, İzmir-Balıkesir Transfer Zone; MCL, Mid-Cycladic Lineament. (b) Geological map of western Anatolia on a digital elevation model (DEM) image showing the distribution of the Miocene sedimentary, volcanic and granitic rocks in the region (modified from geological map of Turkey from GDMRE 2002). The two sedimentary sections of Şen & Seyitoğlu (2009) and one of Kondopoulou *et al.* (2011) documented in the Gediz Graben, Büyük Menderes Graben and Chios are shown as the Zeytinçayı, Eycelli and Chios sections, respectively. Kg, Kozak granite; Ey, Eybek granite; Og, Orhanlı granite; Ag, Alaçamdağ granite; Eg, Eğriçöz granite; Bg, Buldan granite; Sg, Salihli granite; Tg, Turgutlu granite; Kav, Karaburun volcanic suite; Kv, Kocadağ volcanic suite; Av, Armağandağ volcanic suite; Yuv, Yuntdağ volcanic suite; Yav, Yamanlar volcanic suite; Fv, Foça volcanic suite; Cv, Çandarlı volcanic suite; Hv, Hisarpete volcanic series; Bv, Balatçık volcanic series. See online version for colour.

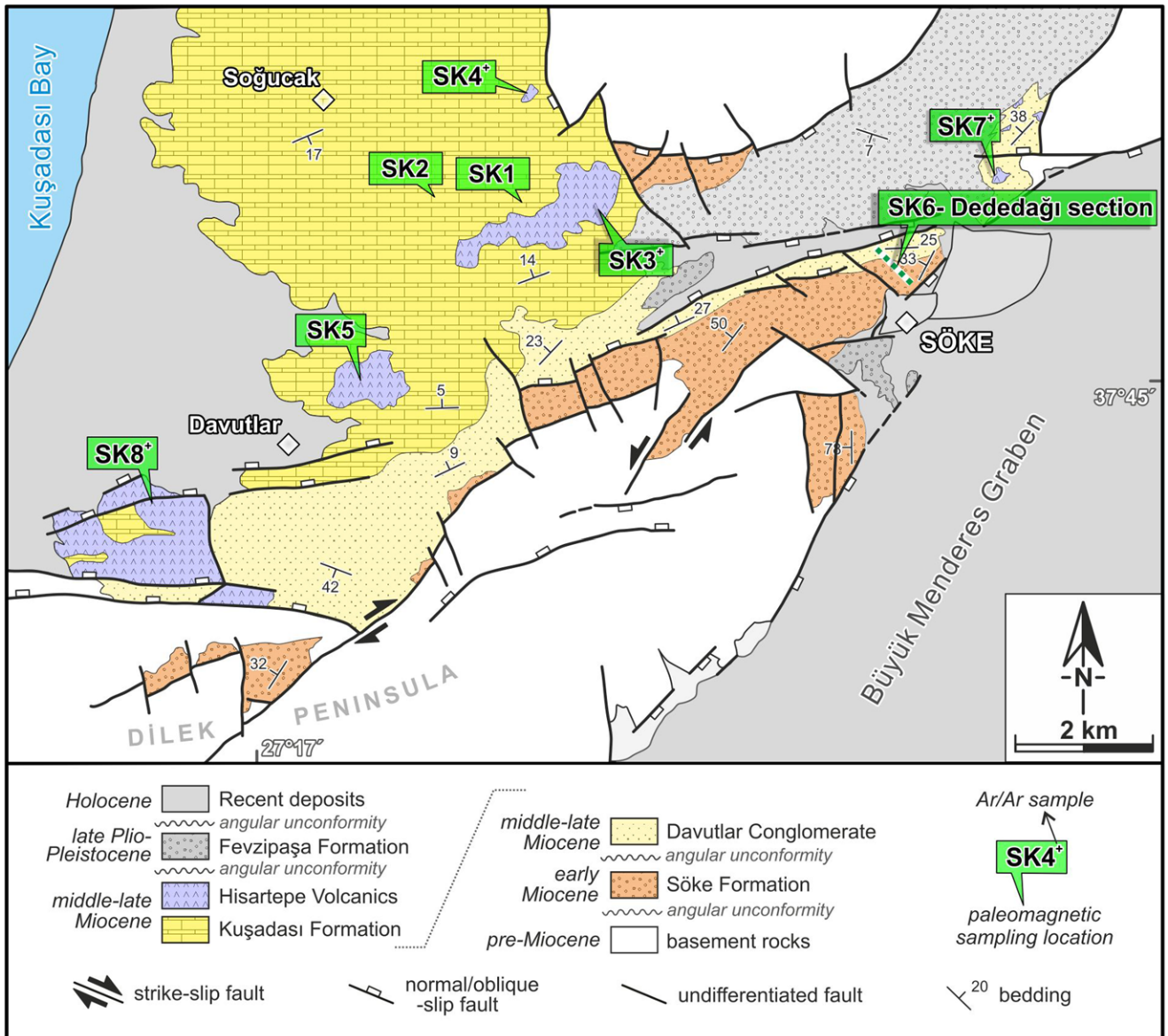


Fig. 2. Detailed geological map of the Söke Basin (simplified from Sümer *et al.* 2013) showing the palaeomagnetic and geochronological sample locations.

with block rotations caused by the North Anatolian Fault Zone (Kissel *et al.* 1993, 2002; Platzman *et al.* 1994, 1998; Piper *et al.* 1996, 1997, 2006, 2010; Tatar *et al.* 1996, 2000, 2002, 2004; Gürsoy *et al.* 1997, 1999, 2003; İşseven & Tüysüz 2006; Kaymakci *et al.* 2007). In addition to these, a large palaeomagnetic database is available from the Aegean Islands and the mainland of Greece (Kissel *et al.* 1986; Avigad *et al.* 1998; Duermeijer *et al.* 1998, 2000; Kondopoulou 2000; van Hinsbergen *et al.* 2004, 2005b, 2007, 2008; Kondopoulou *et al.* 2011; Bradley *et al.* 2013). Additional palaeomagnetic studies relate to the tectonic events in central Anatolia (Gürsoy *et al.* 1997, 1998, 1999, 2003; Piper *et al.* 2002; Kaymakci *et al.* 2003; Meijers *et al.* 2010, 2011; Gülyüz *et al.* 2013; Lefebvre *et al.* 2013; Çinku *et al.* 2015). To shed light on the possible block rotations and the tectonic evolution of western Anatolia, only a few palaeomagnetic studies have been carried out. After the pioneering work of Kissel *et al.* (1987), later studies by Şen & Seyitoğlu (2009), van Hinsbergen *et al.* (2010a), Kondopoulou *et al.* (2011) and Uzel *et al.* (2015) have contributed to the palaeomagnetic database of western Anatolia, addressing the timing and nature of the Aegean–west Anatolian tectonics (Fig. 1b).

According to this literature there seem to be two outstanding questions. (1) What is the driving mechanism of regional extension

in western Anatolia? (2) What is the nature of this extension characterized by large-scale detachments and high-angle normal faults: was it episodic or continuous? In this paper, we specifically address the second question by presenting new palaeomagnetic and $^{40}\text{Ar}/^{39}\text{Ar}$ radio-isotope data from the volcanic and sedimentary rock sequences in the Söke Basin as an important tool to reveal the timing of rotational deformation of the region, and to quantify the vertical block rotations during the Miocene. The palaeomagnetic and geochronological results are integrated with field observations, and the results are compared with other western Anatolian basins for which data are available in the literature. We then discuss the importance of the episodic extension for the region and consequences for the exhumation of core complexes and related basin formation in western Anatolia.

Söke Basin

The Söke Basin is located at the western rim of the Büyük Menderes graben and extends from the Dilek Peninsula in the south to Kuşadası Bay to the north (Figs 1 and 2). The structural architecture, tectono-stratigraphical evolution and late Cenozoic stratigraphy of the Söke Basin was established by Ercan *et al.* (1986), Yılmaz *et al.*

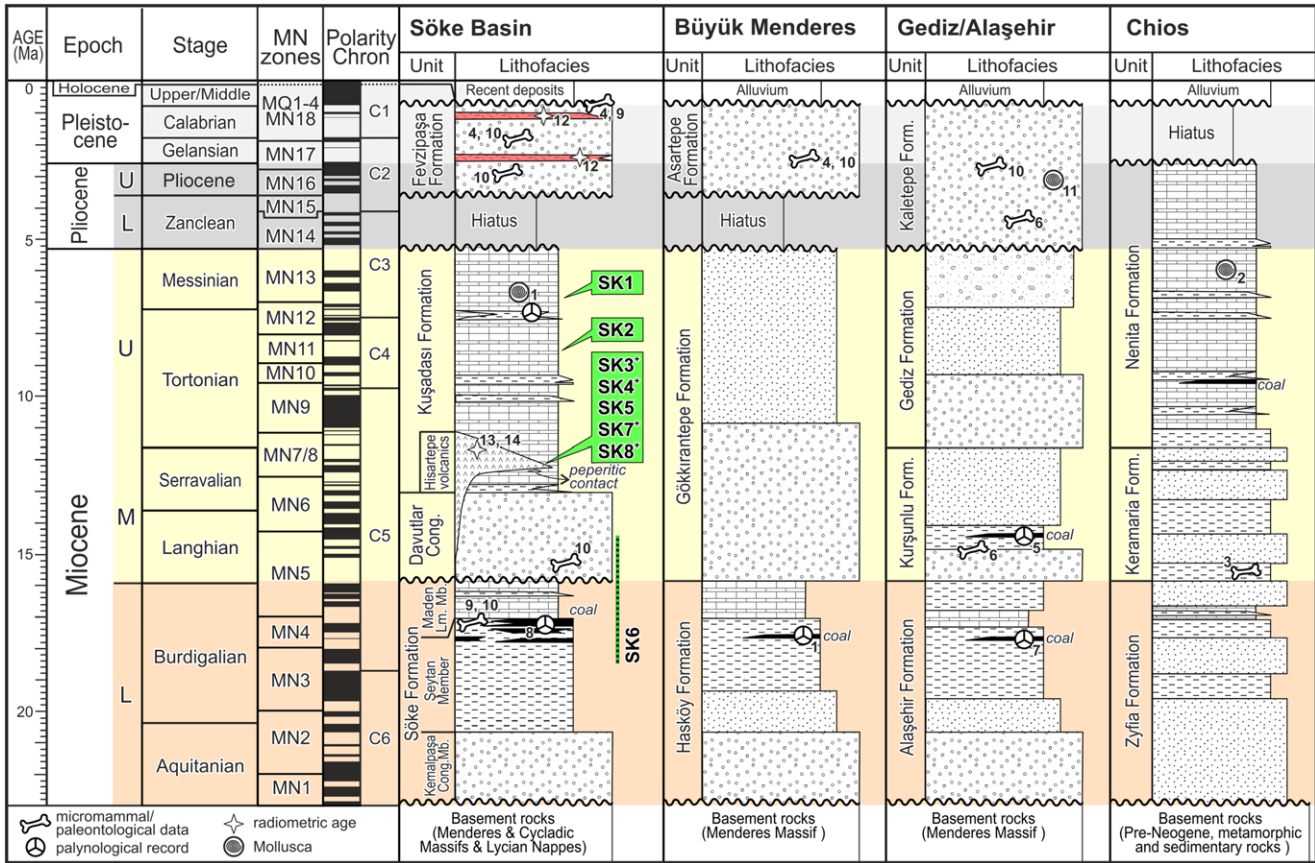


Fig. 3. Stratigraphic sections of Söke Basin (Sümer *et al.* 2012, 2013), Büyük Menderes Graben (Şen & Seyitoğlu 2009; Çiftçi *et al.* 2011), Gediz/Alaşehir Graben (Yazman *et al.* 1998; Çiftçi & Bozkurt 2009; Şen & Seyitoğlu 2009) and Chios (Beseneker 1973; Kondopoulou *et al.* 2011). The mammal zones and magnetic polarity timescale are taken from Lindsay (1997), Steininger (1999) and Hilgen *et al.* (2012). References for age and palaeontological data on the sections: (1) Becker-Platen (1970); (2) Schutt & Beseneker (1973); (3) Koufos *et al.* (1995); (4) Ünay *et al.* (1995); (5) Seyitoğlu & Scott (1996); (6) Şan (1998); (7) Yazman *et al.* (1998); Ediger *et al.* (1996); (8) Akgün & Akyol (1999); (9) Ünay & Göktaş (1999); (10) Sarca (2000); (11) Şen & Seyitoğlu (2009); (12) Sümer *et al.* (2012); (13) Sümer *et al.* (2013); (14) this study.



Fig. 4. Field photographs showing contact relations of the Miocene units. (a) Angular unconformity between the Maden Limestone Member of the Söke Formation and the Davutlar Conglomerate (the continuous white lines indicate bedding of the units; the bold dotted curve indicates the trace of angular unconformity); (b) angular clayey limestone clast observed in the Davutlar Conglomerate derived from Maden Limestone Member; (c) peperitic contact, arrows show the fluidal margin between a lava flow of the Hisartepe volcanic series and the limestone of the Kuşadası Formation (pen 14 cm; person 190 cm).

Middle Miocene unconformity, Söke Basin, Anatolia

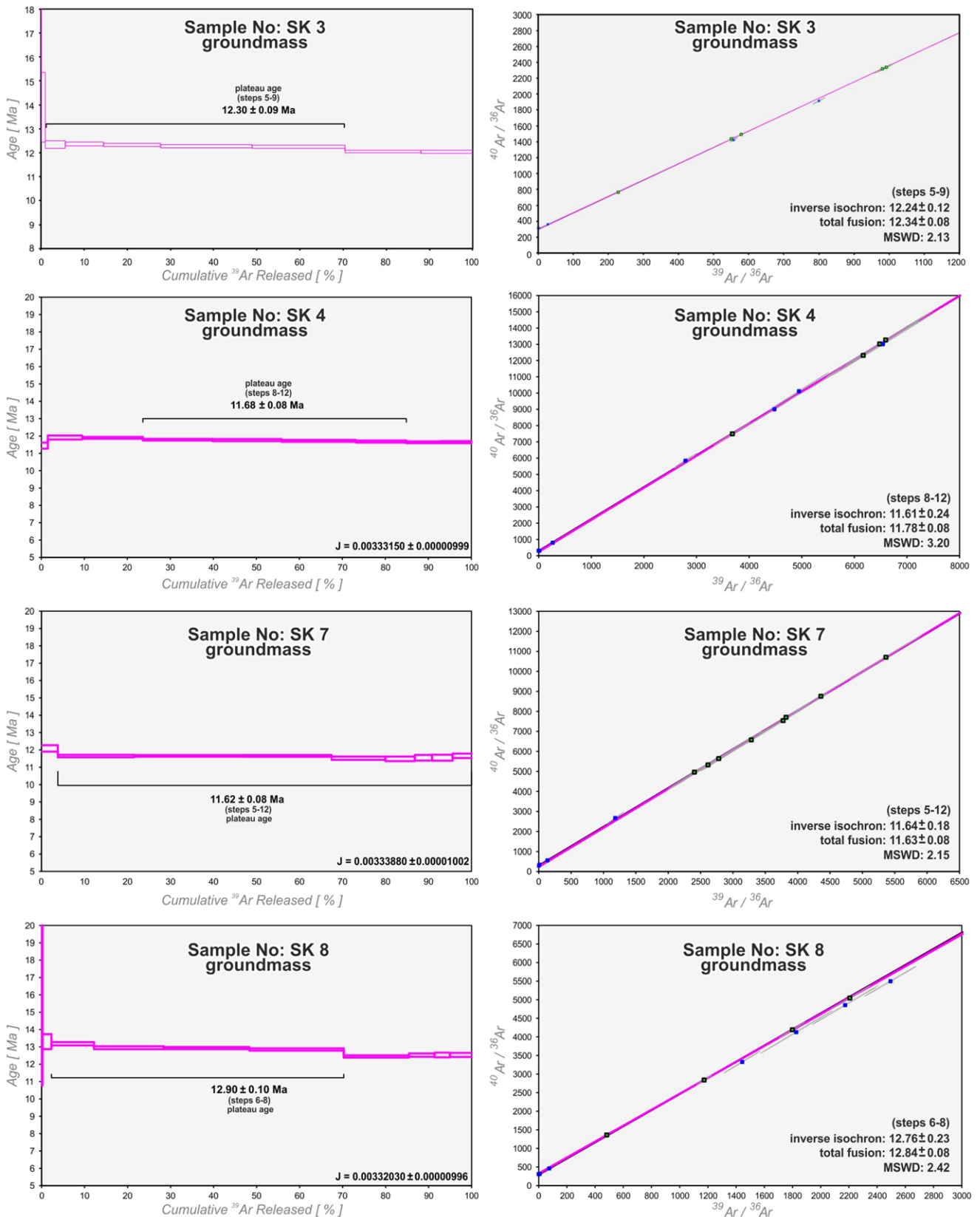


Fig. 5. Apparent age spectra, including age plateau and normal isochron diagrams, for the dated volcanic rocks from the Söke Basin. The width of the bars/steps represents the 2σ analytical error. Ages were calculated using the ArArCalc software developed by Koppers (2002). All $^{40}\text{Ar}/^{39}\text{Ar}$ ages were calculated using Steiger & Jäger (1977) decay constants at the 2σ level and include the analytical error and error in irradiation parameter (J-value). MSWD, mean square weighted deviate.

(1999), Ünay & Göktaş (1999), Sarıca (2000) and Gürer *et al.* (2001, 2009). Recently, Sümer *et al.* (2013) provided evidence for the development and evolution of the basin within a transtensional tectonic environment during the Neogene. According to both

palaeostress analyses (*c.* 300 fault-slip data) and stratigraphic correlation of basin deposits, they suggested that the association of strike-slip and normal faults has controlled the deposition of the Neogene units. The Söke Basin developed on pre-Miocene rock

Table 1. Results of the $^{40}\text{Ar}/^{39}\text{Ar}$ analyses from this study

Sample	$^{40}\text{Ar}^*/^{39}\text{Ar}_K$	$\pm 2\sigma$	Plateau			Steps in plateau	n total	$^{39}\text{Ar}_K$ in plateau		$^{40}\text{Ar}/^{36}\text{Ar}$ intercept inverse isochron		Inverse isochron		Total fusion age	
			age (Ma)	$\pm 2\sigma$	MSWD			(%)	Average $^{40}\text{Ar}^*$ (%)	$\pm 2\sigma$	age (Ma)	$\pm 2\sigma$	age (Ma)	$\pm 2\sigma$	
SK03	2.06546	0.00740	12.30	0.09	2.13	5–9	11	69.4	79.1	303.2	9.9	12.24	0.12	12.34	0.08
SK04	1.95025	0.00770	11.68	0.08	3.20	8–12	12	60.2	97.1	356	197	11.61	0.24	11.78	0.08
SK04	1.94747	0.00607	11.67	0.08	1.64	9–12	12	44.2	96.9	381	115	11.56	0.16	11.63	0.08
SK07	1.93631	0.00668	11.62	0.08	2.15	5–12	12	96.2	95.5	281	120	11.64	0.18	11.63	0.08
SK08	2.16200	0.01029	12.90	0.10	2.42	6–8	12	58.1	92.2	336.3	61.6	12.76	0.23	12.84	0.08

units (basement rocks) consisting of (1) metamorphic rocks of the Menderes and Cycladic metamorphic core complexes, and (2) sedimentary rocks of the Lycian Nappes. A detailed description of the basement rocks is beyond the scope of this paper, and we refer readers to Candan *et al.* (1997), Oberhänsli *et al.* (1998), Dora *et al.* (2001), Okay (2001), Çetinkaplan (2002), Rimmelé *et al.* (2006) and Çakmaköglü (2007) for additional information, but here we summarize the Miocene rock units of the Söke Basin, mainly after Sümer *et al.* (2013).

Miocene stratigraphy

The Miocene stratigraphy of the Söke Basin includes two main rock packages, the Lower and Upper sequences, separated by a major middle Miocene unconformity. The Lower sequence consists of sedimentary rocks of the Söke Formation, whereas the Upper Sequence comprises the Davutlar Conglomerates, the Kuşadası Formation and the Hisartepe volcanic series (Figs 2 and 3). The Söke Formation consists of facies associations ranging from alluvial fan to lacustrine sedimentary rocks intercalated with coal levels up to 3 m thick. The formation is divided into three members that are laterally and vertically gradational (Fig. 3). These are the coarse-grained sedimentary facies (the Kemalpaşa Conglomerate Member), the coarse- to fine-grained clastic rocks (the Şeytan Member) and lacustrine carbonates (the Maden Limestone Member). Sümer *et al.* (2013) reported that the maximum exposed thickness of the Söke Formation is *c.* 250 m.

In all previous studies (e.g. Ünay & Göktaş 1999; Gürer *et al.* 2001; Sümer *et al.* 2013) that have focused on the Miocene evolution of the Söke Basin, the stratigraphic contact between the Lower and the Upper sequences is described as a major angular unconformity (Fig. 3). This middle Miocene unconformity contact can be seen clearly between the steeply dipping Söke Formation and the gently dipping Davutlar Conglomerate exposed at the east of Davutlar village (Fig. 4a). Along a valley section, a 25–30° angular difference is clearly visible between the Söke Formation (the Maden Limestone Member) at the bottom, with alternations of mudstone, limestones and clayey limestone dominant facies, and the overlying Davutlar Conglomerate, with thick basal conglomerate beds grading upward into a cross-bedded, fining and thinning upward clastic sequence. On the basis of several micro-mammal (rodent) fauna (Ünay & Göktaş 1999; Sarıca 2000) and sporomorph assemblages (Akgün & Akyol 1999), the age of the Söke Formation is considered as early Miocene (Sümer *et al.* 2013).

The Upper sequence begins with the Davutlar Conglomerates (Fig. 3). It consists mainly of well-rounded marble and schist clasts from the crystalline basement, and angular clasts derived from the Söke Formation (Fig. 4b). The unit interfingers laterally and vertically with sandstone, mudstone, calcareous siltstone, clayey limestone and calcareous claystones of the Kuşadası Formation (Fig. 3). The Hisartepe volcanic series is exposed between Söke and Davutlar villages, and the outcrops are mainly aligned in a NE–SW trend (Fig. 2). The unit comprises dark-coloured volcanic domes, dykes,

lavas and intrusive bodies in basaltic andesite, trachyandesitic and dacitic rocks. Ercan *et al.* (1986) reported that the volcanic rocks exposed in the Söke region are calc-alkaline in nature, mainly of crustal origin and only partly sourced from deeper (mantle) material. At the contact between the Kuşadası Formation and the Hisartepe volcanic series, some peperitic textures are observed in the field (Fig. 4c). These textures are characterized by flow-aligned elongate vesicles with fluidal margins, as well as trachyandesitic lobes, and are thought to be closely associated with magma compositions that would allow easier penetration into the host sediment (Dadd & van Wagoner 2002). This wet sediment–hot lava interaction means that the beginning of deposition of the Kuşadası Formation must therefore be simultaneous with the onset of the Hisartepe volcanic series in the basin. The Hisartepe volcanic rocks were first dated by Ercan *et al.* (1986) to 6.99 ± 0.22 Ma using the K/Ar (whole-rock) method. Recently, Sümer *et al.* (2013) reported a significantly older $^{40}\text{Ar}/^{39}\text{Ar}$ age of 12.31 ± 0.09 Ma (groundmass plateau age). Combining these ages with published radio-isotope age data and palaeontological studies based on micro-mammal faunas (Ünay & Göktaş 1999; Sarıca 2000), ostracods, gastropods and sporomorph assemblages (Becker-Platen 1970), we suggest that the age of the Upper Sequence is mainly middle–late Miocene (*c.* 15–7? Ma).

The younger units of the Söke area are the Fevzipaşa Formation and Recent deposits resting unconformably on the Miocene successions of the basin (Figs 2 and 3). The Fevzipaşa Formation comprises an alternation of conglomerates, sandstones and mudstones intercalated with lacustrine limestones and two conspicuous tuff layers, which are observed at the lower and middle parts of the formation. The age of the formation was recently documented as late Pliocene–Pleistocene based on correlation of published micro-mammal identifications (Ünay *et al.* 1995; Ünay & Göktaş 1999; Sarıca 2000) and radio-isotope ages from interlayered tuffs (Sümer *et al.* 2012) (Fig. 3). The Recent deposits comprise coarse-grained clastic sediments, which are deposited in marginal alluvial or colluvial fans and alluvial-apron deposits, and relatively finer grained sediments, which accumulated in fluvial and alluvial environments (Figs 2 and 3).

$^{40}\text{Ar}/^{39}\text{Ar}$ geochronology

Sampling and analytical techniques

To establish the temporal constraints on the palaeomagnetic results, we performed new $^{40}\text{Ar}/^{39}\text{Ar}$ age determinations on three lava flows that were collected from Asartepe Hill, Yaylaköy and Hisartepe Hill (SK4, SK7 and SK8), respectively (Fig. 2). Here we date the volcanic rocks, which are mainly composed of dark-coloured basaltic andesite, trachyandesite and dacitic lavas, domes and dykes. The samples consist of euhedral sanidine, biotite, hornblende and quartz phenocryst assemblages in mainly plagioclase microlites and volcanic glass matrix. The rock samples were processed at Free University (VU) Amsterdam (the Netherlands). The samples were crushed and washed, followed by density separation to remove the

Middle Miocene unconformity, Söke Basin, Anatolia

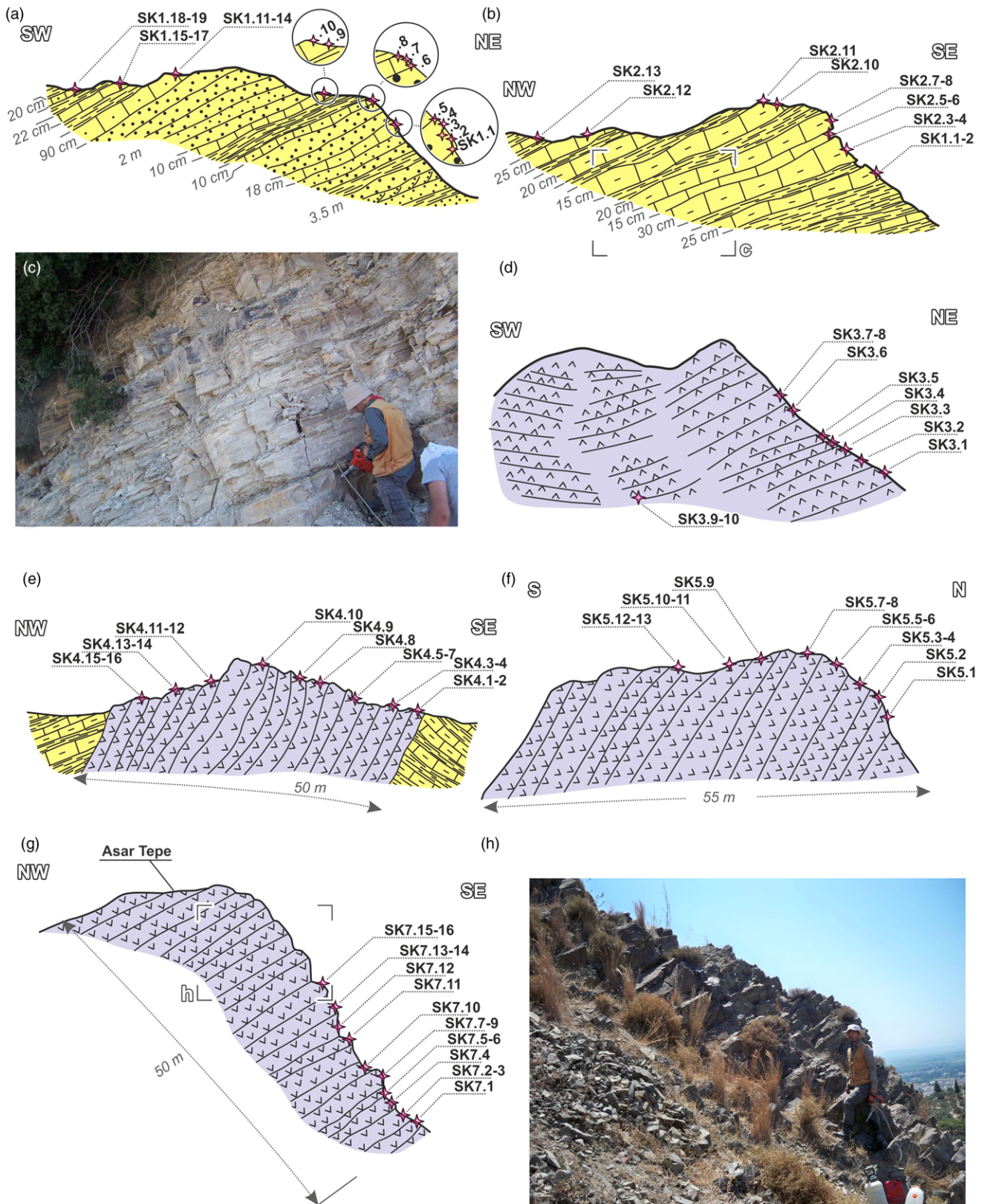


Fig. 6. Geological field cross-sections and photographs showing stratigraphic positions of the palaeomagnetic samples within the Söke Basin. (a, c) SK1, (b) SK2, (d) SK3, (e) SK4, (f) SK5, (g, h) SK7.

phenocrysts. Hand-picked groundmass separates were wrapped in Al foil and irradiated with Fish Canyon tuff sanidine as a neutron fluency monitor at the Cd-shielded P3 position of the High Flux Reactor in Petten (Netherlands) for 12 h. After irradiation, the samples were loaded in a Cu tray and analysed using a Synrad 48-5 CO₂ laser and custom beam delivery system for laser single fusion

(standard) and incremental heating. The samples were purified in an in-house designed sample clean-up line fitted with NP10 and ST172 getters and analysed on a MAP215-50 noble gas mass spectrometer fitted with a Balzers SEV217 SEM detector. The ages were calculated relative to 28.201 ± 0.08 Ma for Fish Canyon tuff sanidine (Kuiper *et al.* 2008) and Min *et al.* (2000) decay constants.

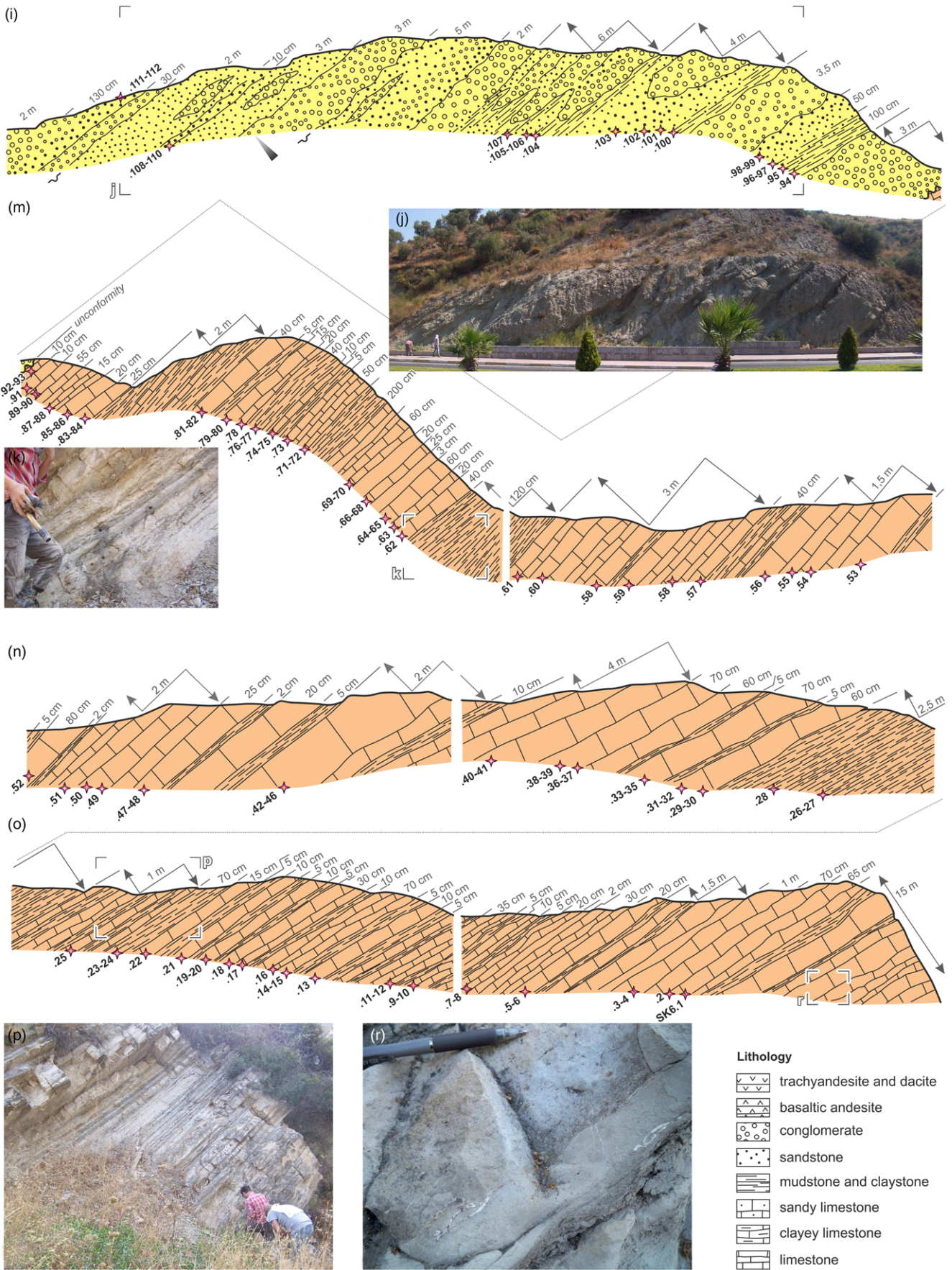


Fig. 6. Continued. (i–r) SK6. See Figures 2 & 3 for the geographic & stratigraphic positions of the sampling.

Correction factors for neutron interference reactions were $(2.65 \pm 0.15) \times 10^{-4}$ for $(^{36}\text{Ar}/^{37}\text{Ar})\text{Ca}$, $(7.33 \pm 0.68) \times 10^{-4}$ for $(^{39}\text{Ar}/^{37}\text{Ar})\text{Ca}$, $(1.139 \pm 0.006) \times 10^{-2}$ for $(^{38}\text{Ar}/^{39}\text{Ar})\text{K}$, and $(0.13 \pm 0.15) \times$

10^{-2} for $(^{40}\text{Ar}/^{39}\text{Ar})\text{K}$. The $^{40}\text{Ar}/^{36}\text{Ar}$ ratio of 295.5 determined by Nier (1950) was used in the calculations. All errors are reported at 2σ level and include analytical errors in sample and error in J-value.

Table 2. Details of palaeomagnetic data from this study

Sample	Latitude (°N)	Longitude (°E)	Age	<i>n</i>	ChRM directions, geographical										Strike/dip	ChRM directions, tectonic									
					<i>n</i> ₄₅	<i>D</i>	<i>I</i>	ΔD_x	ΔI_x	<i>k</i>	α_{95}	<i>K</i>	$A_{95\min} < A_{95} < A_{95\max}$	<i>N</i> ₄₅		<i>D</i>	<i>I</i>	ΔD_x	ΔI_x	<i>k</i>	α_{95}	<i>K</i>	$A_{95\min} < A_{95} < A_{95\max}$		
SK01	37.7706	27.3373	Middle-late Miocene	15	12	359.2	55.4	12.5	9.9	34.4	7.5	19.4	$4.4 < 10.1 < 17.1$	009/18	12	25.2	54.4	11.3	9.3	34.4	7.5	23.0	$4.4 < 9.2 < 17.1$		
SK02	37.7995	27.3218	Middle-late Miocene	16	15	32.4	55.0	7.0	5.6	69.8	4.8	50.3	$4.2 < 5.7 < 15.6$	249/18	15	15.3	43.9	7.5	8.7	40.1	6.1	32.6	$4.1 < 6.8 < 14.9$		
SK03	37.7734	27.3477	Middle-late Miocene	10	9	49.4	59.2	10.9	7.4	63.4	6.5	39.1	$5.0 < 8.3 < 20.5$	249/23	9	23.3	46.4	8.7	9.4	63.4	6.5	45.4	$5.0 < 7.7 < 20.5$		
SK04	37.7879	27.3372	Middle-late Miocene	16	15	81.7	21.9	4.8	8.5	46.1	5.7	66.1	$4.1 < 4.7 < 14.9$	205/60	15	32.0	60.0	10.3	6.8	46.1	5.7	25.2	$4.1 < 7.8 < 14.9$		
SK05*	37.7412	27.3112	Middle-late Miocene	13																					
SK06	37.7227	27.3972	Middle-late Miocene	22	19	7.5	49.5	10.9	10.6	17.3	8.3	13.8	$3.7 < 9.4 < 12.8$	269/25	21	7.9	27.4	8.3	13.6	13.7	8.9	16.5	$3.6 < 8.1 < 12.0$		
SK07	37.7725	27.4180	Middle-late Miocene	16	7	262.5	-31.9	3.4	5.1	246.8	3.8	355.6	$3.2 < 5.5 = A_{95\min}$	214/55	7	207.0	-55.5	6.1	4.9	246.8	3.8	149.9	$4.9 < 5.5 = A_{95\min}$		
SK08*	37.7412	27.3112	Middle-late Miocene	8																					
Mean	SK01-04		Middle-late Miocene	57	43	54.2	48.2	8.7	8.8	10.4	7.1	9.3	$2.7 < 7.6 < 7.7$		51	23.1	51.7	5.0	5.6	32.1	2.5	23.0	$2.5 < 4.3 < 6.9$		
Mean	SK06 (early Miocene)		Early Miocene	125	122	352.1	53.2	3.6	3.1	29.5	2.4	19.5	$1.8 < 3.0 < 4.0$	209/33	125	331.9	28.8	2.4	3.8	26.9	2.3	31.8	$1.7 < 2.3 < 3.9$		
Mean	SK06 (early Miocene), <i>E/I</i>		Early Miocene	125											125	331.6	40.6	2.6	3.3	25.1	2.6	28.3	$1.7 < 2.4 < 3.9$		

n, number of measured and interpreted samples; *n*₄₅, number of samples after application of a fixed cut-off (45°); *D*, declination; *I*, inclination; ΔD_x (ΔI_x), corresponding error in declination (inclination); *k* is precision parameter and α_{95} is cone of confidence of the ChRM distribution; *K* is precision parameter and A_{95} is cone of confidence of the VGP distribution; $A_{95\min}$ and $A_{95\max}$ correspond to the confidence envelope of Deenen *et al.* (2011, 2014). If A_{95} falls within this envelope the distribution probably represents palaeosecular variation. If $A_{95} < A_{95\min}$ the distribution is too tight and represents a spot-reading of the field, as is the case for SK7. All values are given before (geographical) and after (tectonic) correction for bedding tilt (strike/dip). *Sites removed from further analysis because of lightning-induced directions (SK8) or no interpretable results (SK5).

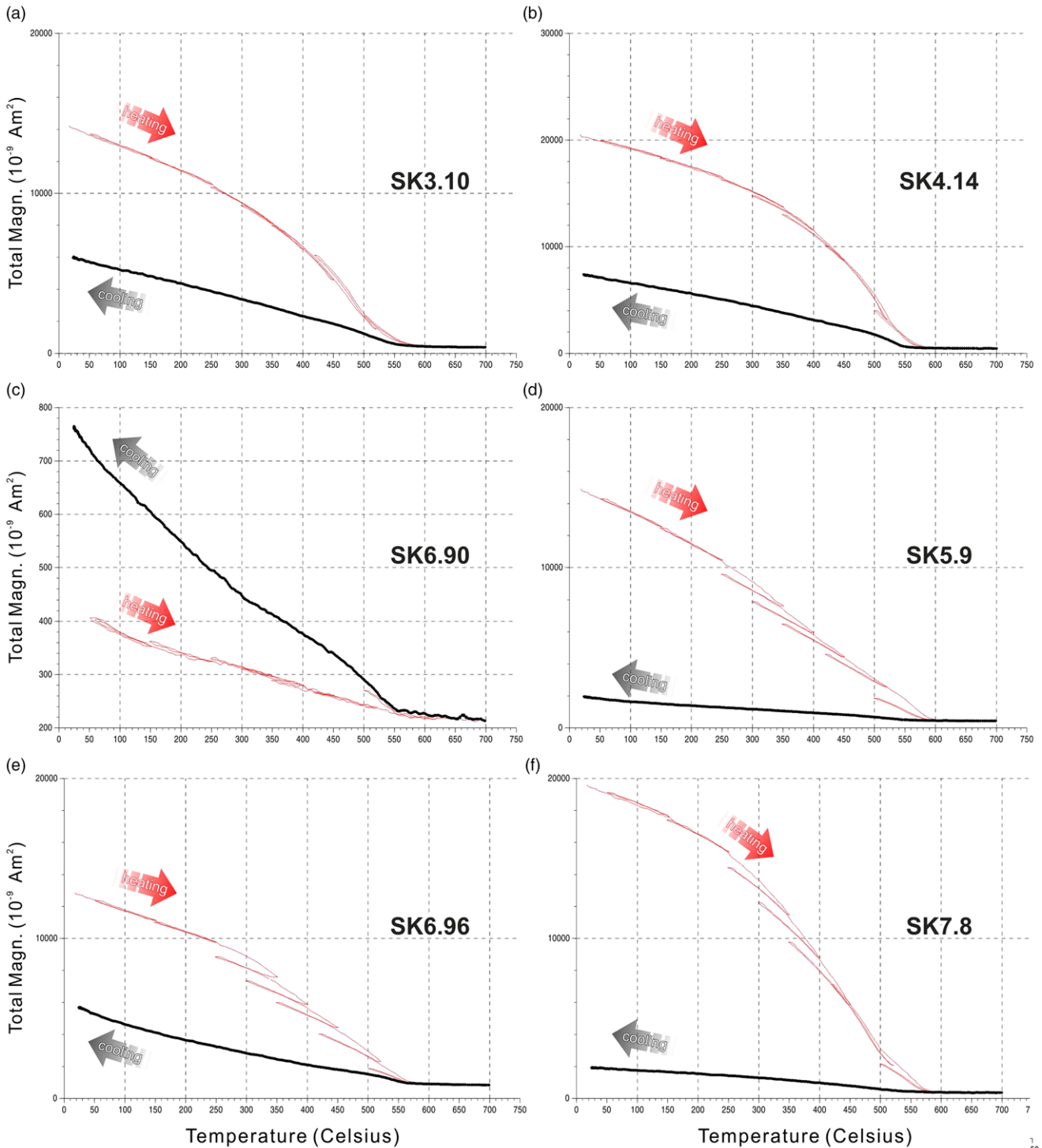


Fig. 7. Thermomagnetic curves measured on a Curie balance (Mullender *et al.* 1993) for some representative samples of the Söke Basin. Curves indicate heating and cooling stages of measurements.

Reliable plateau ages are defined as comprising at least three contiguous steps corresponding to at least 50% of the total ^{39}Ar released and showing no significant slope, with the individual step ages agreeing within 2σ errors with the weighted mean age of the plateau segment (Fig. 5 and Table 1). Full analytical data are available in the Supplementary Material.

Geochronological results

Sample SK4 yields an age spectrum that apart from the initial steps slightly decreases in age. The last five steps yield a weighted mean

age of 11.68 ± 0.08 Ma and contain $>60\%$ of the $^{39}\text{Ar}_K$ released but the mean square weighted deviate (MSWD; a measure for explaining observed scatter) of 3.20 points towards some scatter beyond analytical uncertainties only. The ‘plateau’ age does not overlap with the total fusion age of 11.78 Ma if only analytical errors are considered. $^{40}\text{Ar}/^{36}\text{Ar}$ intercepts are not well constrained, but do not point towards excess argon issues. An alternative interpretation is an age plateau comprising the last four steps yielding 11.67 ± 0.08 Ma with MSWD 1.64, but including only 44% of the $^{39}\text{Ar}_K$ released and therefore not strictly following our plateau criteria (Fig. 5 and Table 1).

Sample SK7 produced a nearly flat age spectrum of 11.62 ± 0.08 Ma including steps 5–12, containing >96% of the $^{39}\text{Ar}_K$ released, and indistinguishable from the total fusion age of 11.63 ± 0.08 Ma (Fig. 5 and Table 1). The $^{40}\text{Ar}/^{36}\text{Ar}$ isochron intercepts are poorly constrained but do not give evidence for excess argon.

Sample SK8 yields a plateau age of 12.90 ± 0.10 Ma with no evidence for excess argon. The total fusion age overlaps with the plateau age (Fig. 5 and Table 1). $^{40}\text{Ar}/^{39}\text{Ar}$ data from the Hisartepe Hill as described by Sümer *et al.* (2013) are here reported as sampling location SK3 (Fig. 2), and yield a plateau age of 12.33 ± 0.09 Ma. Isochrons do not show evidence for excess argon, and the plateau age is the preferred age (Fig. 5 and Table 1).

Palaeomagnetism

Sampling procedures

Palaeomagnetic samples were collected by drilling standard cores using gasoline-powered drills. At least 11 cores at each site were taken, after removing the weathered surface (sediments) to reach a fresh outcrop. Sample orientations were measured with a magnetic compass (plus sun compass for lavas). The sample core orientations as well as the bedding tilts were corrected for present-day declination (typically 4°E for the entire sampling period). The measurements and analysis of the samples were carried out at the Fort Hoofddijk Palaeomagnetic Laboratory of Utrecht University (Netherlands).

Sampling localities

For the purpose of understanding the rotational history of the Söke Basin, we collected *c.* 250 sample cores from eight localities, SK1 to SK8, covering the Miocene time interval (Figs 2 and 6). Samples SK1, 2 and 6 were collected from sediments, whereas SK3, 4, 5, 7 and 8 were collected from volcanic rocks. The latter samples have also been dated with the $^{40}\text{Ar}/^{39}\text{Ar}$ method. Sampling details are given below and results are summarized in Table 2.

Sites SK1 and SK2 are in sediments from the Kuşadası Formation, located in the centre of the basin, comprising 19 and 13 palaeomagnetic samples (SK1.1–19 and SK2.1–13), respectively. Sediments are pale grey sandy limestone, greenish grey mudstone and grey sandstone (Fig. 6a–c). Hisartepe volcanic rocks are exposed in isolated outcrops between Söke and Davutlar and were sampled at four sites: SK3, SK4, SK5 and SK7 (Fig. 2). Sixty-three samples were collected from these sites with basaltic and dacitic composition (SK3.1–10, SK4.1–16, SK5.1–13, SK7.1–16 and SK8.1–8) in stratigraphic order (Fig. 6d–h). Along the Dededağ section (SK6), sampling was performed along a line starting from Söke town and continued upwards in a NW direction. The basal part of SK6 comprises early Miocene sedimentary rocks of the Söke Formation (SK6.1–93; Fig. 6k–p), whereas the upper part covers the middle–late Miocene volcano-sedimentary rocks of Kuşadası Formation (SK6.94–107; Fig. 6i and j). At the base, buff lacustrine limestone, greenish grey fossil-rich (mostly gastropod) laminated mudstone beds of the Söke Formation are sampled. In the upper part, above the angular middle Miocene unconformity, the Kuşadası Formation is composed mainly of coarse-grained conglomerate and sandstone alternations; samples were collected from the fine-grained levels intercalated within the sandstone beds, and from mudstones.

Measurements and analyses

The palaeomagnetic samples were demagnetized using alternating field (AF) and thermal (TH) progressive stepwise demagnetization. A single core often provided multiple specimens (for both TH and AF analysis). Thermal demagnetization was carried out in a magnetically shielded oven, with varying steps from 10 to 50°C up to a maximum of 645°C. AF demagnetization was carried out with

increments of 3–20 mT, up to a maximum of 80 or 100 mT. The natural remanent magnetization (NRM) of all samples was measured on a 2G Enterprises horizontal 2G DC SQUID cryogenic magnetometer (noise level 2×10^{-12} Am²). For AF demagnetization, an in-house developed robot assisted and fully automated 2G DC SQUID cryogenic magnetometer was used. The temperatures used for TH demagnetization ranged from 120 to 630° for both volcanic and sedimentary sites; AF demagnetization steps ranged from 1 to 100 mT with small steps (3 or 5 mT) for lower fields up to 40 mT, and 10 mT for higher fields. Demagnetization diagrams of the NRM were plotted and interpreted as orthogonal vector diagrams (Zijderveld 1967; Kirschvink 1980).

To determine characteristic remanent magnetization (ChRM) directions, results from five to eight successive temperature or AF steps were taken. Fisher statistics (Fisher 1953) were used to calculate directional ChRM and virtual geomagnetic pole (VGP) means. Because the scatter of palaeomagnetic directions induced by secular variation of the Earth's magnetic field is circular at the poles but gradually becomes more ellipsoid towards the equator (Tauxe & Kent 2004), we determined the VGP distributions and their means, and calculated the corresponding dispersion and cone of confidence (K, A_{95}). Successively, a fixed 45° VGP cut-off was applied and the errors in declination (ΔD_x) and inclination (ΔI_x) were calculated from A_{95} following Butler (1992). For sedimentary sites, we used the method of Deenen *et al.* (2011) to determine an *n*-dependent $A_{95\text{min}}$ and $A_{95\text{max}}$; if A_{95} lies between these two values the VGP scatter can be explained by secular variation. The tilt test follows the eigenvalue approach of Tauxe & Watson (1994); we used 1000 bootstraps. To correct for a possible shallowing of inclination in sediments caused by compaction during burial, we used the elongation/inclination (*E/I*) method of Tauxe & Kent (2004), provided we had enough samples to do so meaningfully (*n* > 100). For all statistical palaeomagnetic analyses, we used Paleomagnetism.org, which is an open-source and platform-independent portal (Koymans *et al.* 2016). The export file is provided in the Supplementary Material. This file can be uploaded to Paleomagnetism.org in the Statistics Portal (under Advanced Methods – Import Application Save).

Palaeomagnetic results

According to the results of Curie balance analyses, the main carrier of magnetic properties in the Miocene rocks of the Söke Basin appears to be exclusively magnetite (Fig. 7). In most cases, the thermomagnetic curves display a well-shaped curve that is fully reversible up to 250°C in all cases, and reversible up to higher temperatures of nearly 580°C in many cases (Fig. 7a–c). In other cases, between 300 and 580°C some of the magnetite oxidizes or is demagnetized, as the cooling curves show an increasing lower magnetization (Fig. 7d–f). The Curie temperature is typically around 560–580°C, pointing to the main magnetic mineral being (low-Ti) magnetite. Upon heating to 700°C the final cooling curve is no longer reversible, in nearly all cases the magnetite has been oxidized and the cooling curve is significantly lower than the heating curves, except in some sedimentary samples (Fig. 7c, sample SK6.90) where apparently some new magnetite has been created. There is no sign of Fe sulphides in the sediments. Demagnetization analysis also supports that the principal magnetic carrier of the ChRM in the samples is magnetite, evidenced by maximum unblocking temperatures of 500–580°C and unblocking coercivities ranging between *c.* 30 and 90 mT. Only in site SK1 samples are maximum unblocking temperatures lower (Fig. 8a).

Examples of orthogonal vector diagrams (Zijderveld 1967) and equal area projections of the ChRM of all sites are presented in Figure 8. The sediment specimens from the Söke Basin show that the main palaeomagnetic directions are generally obtained at

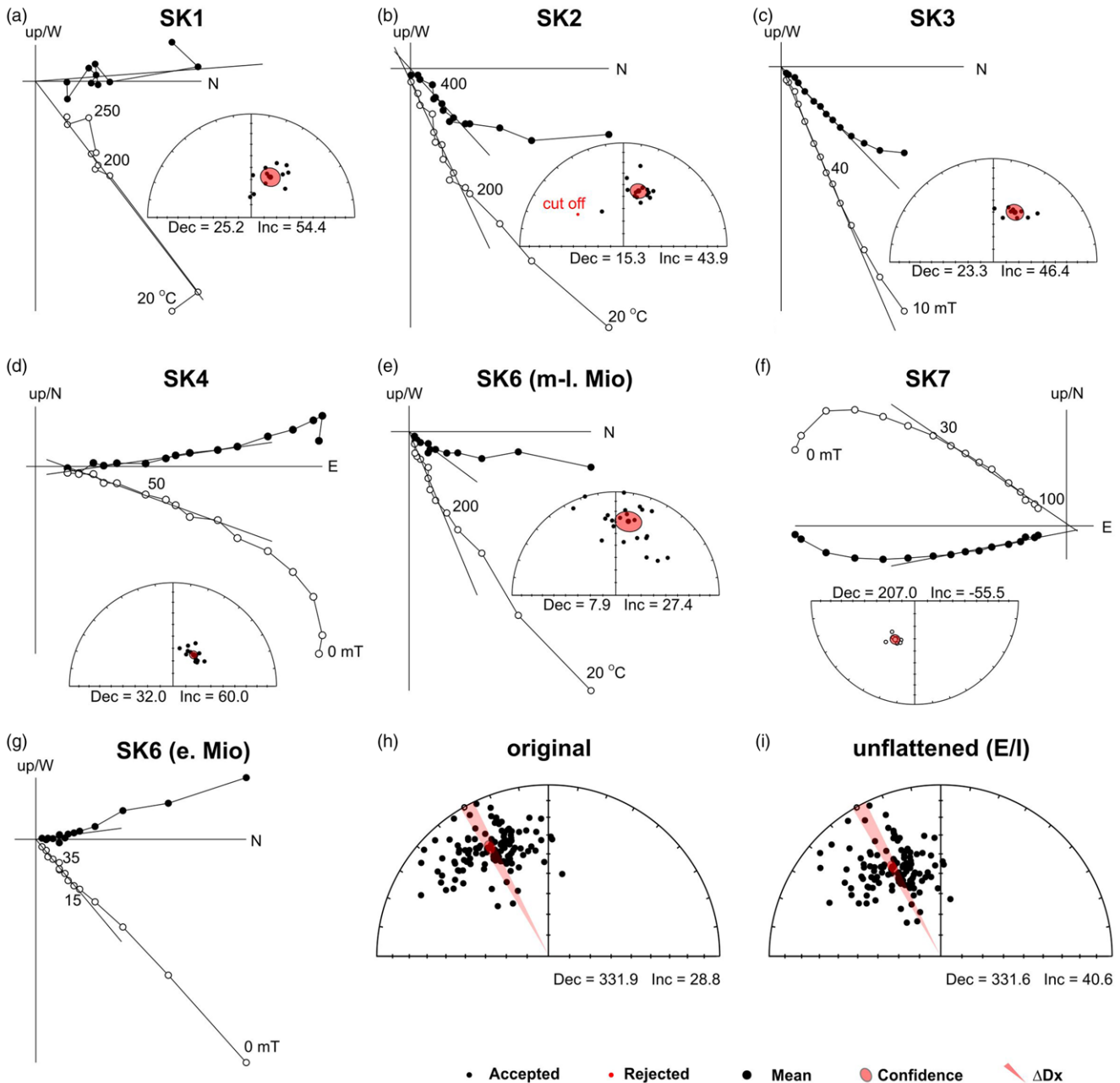


Fig. 8. (a–g) Demagnetization diagrams (Zijderveld 1967) for representative samples; closed (open) circles indicate the projection on the horizontal (vertical) plane. Alternating field ($^{\circ}\text{C}$) and thermal (mT) demagnetization steps are indicated. Equal area projections of the ChRM directions for sites from the Söke Basin; open (closed) symbols denote projection on upper (lower) hemisphere. (h, i) Equal area projections of SK6 (early Miocene) showing the ChRM directions before and after the E/I inclination shallowing correction of Tauxe & Kent (2004). Small grey circles indicate the directions rejected after applying a fixed (45°) cut-off.

temperatures between 180 and 400°C (or 20 and 60 mT, in alternating field demagnetization), after removal of a low-temperature or low-coercivity viscous component. For the volcanic samples, the main component is obtained between 200 and 530°C (or 20–90 mT). On the basis of the quality and reliability of the results, six localities were accepted for further analysis (Fig. 8 and Table 2). Two sites were not accepted for further analysis because samples were affected by lightning strikes (SK8) as was evident from the demagnetization behaviour, or had a too low intensity (SK5).

In the case of SK7, the mean has a k value of 247 and an A_{95} that is lower than $A_{95\text{min}}$ (Deenen *et al.* 2011, 2014). Hence, the mean direction has not averaged secular variation. The other volcanic sites (SK3 and SK4) have A_{95} values that suggest that we have sufficiently sampled secular variation (Table 2). The accepted results display a clear pattern of rotations: on average clockwise (CW) for the younger middle to late Miocene localities, and counterclockwise (CCW) for

the older early Miocene locality (Fig. 8 and Table 2). The older rotation is documented along the basal part of the Dededađı section (SK6) and is derived from early Miocene sedimentary rocks of the Söke Formation; the results show a substantial $28.4^{\circ} \pm 2.6^{\circ}$ CCW (net) rotation. Because the mean inclination is lower than is expected for this location and age (original $I = 28.8^{\circ}$), we used the E/I method (Tauxe & Kent 2004) on these early Miocene sediments, because at this site we have a sufficient number of analyses ($n = 122$ after the 45° cut-off). It shows that the inclination becomes significantly steeper (Fig. 9) at $I = 41^{\circ}$ (ranging from 33.3 to 48.7° at the 95% bootstrap error level), but is still lower than may be expected at this age and latitude. The original and unflattened distributions are shown in Figure 8h and i. The younger locations, in contrast, all show CW rotations (Table 2). Because SK7 represents a single spot reading, we did not use this site. Site SK6 has an anomalously low inclination upon bedding tilt correction, which means that the magnetization may

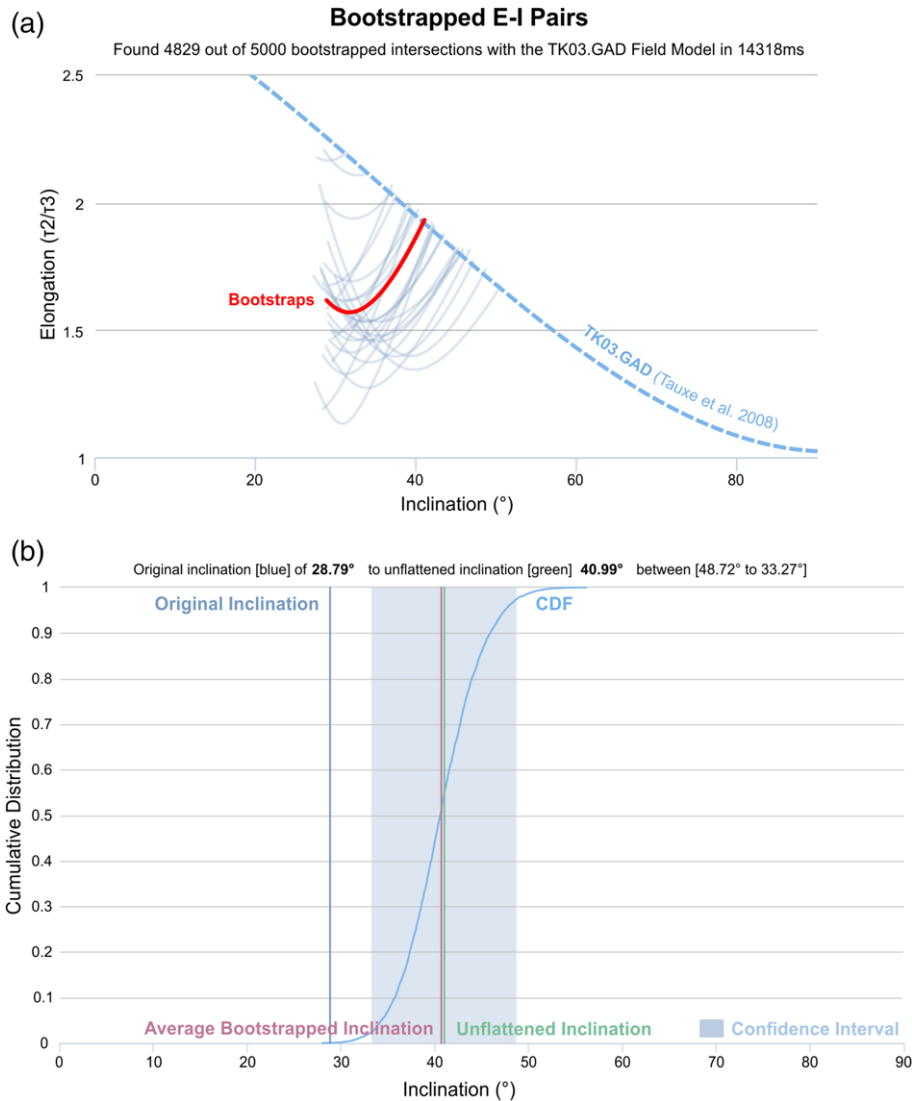


Fig. 9. (a) Elongation v. inclination of the early Miocene data with increasing flattening factor CDF. For every value of f (range 0.3 – 1.0) 5000 bootstraps of the dataset are taken; examples of (25) bootstraps are shown as light grey curves. (b) Bootstrap cumulative distribution functions (CDF) of the unflattened inclinations, illustrating the inclination before and after unflattening, the mean of the bootstraps that intersect with the model, and the 95% confidence interval (Tauxe & Kent, 2004; Tauxe *et al.*, 2008).

have been acquired after folding. We do not know the age of folding, and hence we did not use this site in our final assessment of the tectonic rotation of the younger sites. Consequently, we used the accepted younger sites (SK1 – 4) to perform a bootstrapped tilt test (Tauxe & Watson 1994) using the portal Paleomagnetism.org (Koymans *et al.* 2016). Using 1000 bootstraps, we found that at 100% untilting (within the range 90 – 110% at the 95% error level) we have a positive tilt test (Fig. 10). The mean CW rotation for the younger sediments is $23^{\circ} \pm 5.0^{\circ}$ (Table 2).

Discussion

Distribution of palaeomagnetic directions

Volcanic rocks cool within weeks to years depending on thickness and volume of the volcanic material (Dosseto *et al.* 2011). The fast cooling leads to them recording a spot reading of the geomagnetic field, typically shown by high k values or low A_{95} (Deenen *et al.* 2011). Therefore, sufficiently averaging the palaeosecular variation requires many lava flows (Biggin *et al.* 2008a,b). A sufficiently thick sedimentary sequence, however, represents thousands of years and sufficiently averages out palaeosecular variation. Here we choose a strategy to sample both sediments and lava flows to arrive at a reliable dataset that adds to the existing, but limited, rotational data available for western Anatolia. In this study, it appears that this approach did not work for site SK7, where palaeosecular variation

was not sufficiently averaged out. Another source of error in determining vertical-axis rotations in western Anatolia could also be the size of the rotating blocks and the presence of multiple phases of deformation (e.g. Uzel *et al.* 2013). To see the lateral continuity of the Miocene rotational history and the consequences within west Anatolian grabens, we attempt to correlate our well-dated palaeomagnetic data from the Söke Basin with published magnetostratigraphic sections (Şen & Seyitoğlu 2009) including the same time interval (Figs 3 and 11). Additionally, we discuss our results in the context of recently published palaeomagnetic data (van Hinsbergen *et al.* 2010a; Kondopoulou *et al.* 2011; Uzel *et al.* 2015) with the aim of understanding the role of the middle Miocene interruption in basin formation within the following domains.

The Gediz Graben.

The Zeytinçayı section is located some 4 km west of Alaşehir, at the southern rim of the Gediz Graben (Figs 1b and 11a). It includes two correlative sections called the river and road sections (Şen & Seyitoğlu 2009). The composite section covers the early–middle Miocene transition characterized by the stratigraphic contact between the Alaşehir and Çaltılık (or Kurşunlu) Formations (Fig. 3). The Zeytinçayı section begins with grey–green laminated clays, mudstones and a few sandstones belonging to the upper part of the Alaşehir Formation; then continues with pinkish-red clays, sandstones and conglomerates of the Kurşunlu Formation (Şen &

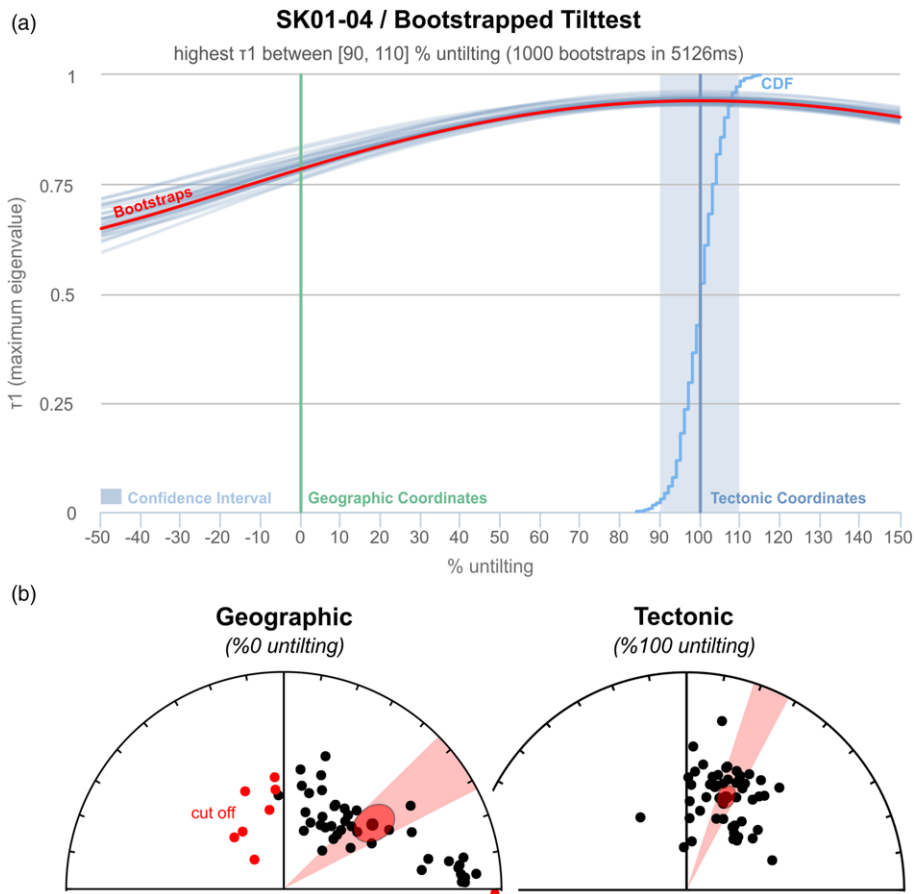


Fig. 10. (a) Tilt test of sites SK01, SK02, SK03 and SK04 (see Table 2) showing the bootstrap cumulative distribution function of stepwise untilting (from -50 to $+150\%$) according to Tauxe & Watson (1994). The mean of 1000 bootstraps is shown (bold curve) with examples of 25 bootstraps (grey curves) and the bootstrap 95% confidence interval (shaded). The confidence interval ($90 - 110\%$) includes 100% untilting, so the tilt test is positive. (b) Equal area projections of the magnetic directions in geographical (left) and tectonic (right) coordinates.

Seyitoğlu 2009). Despite continuing arguments regarding the Miocene stratigraphy of the Gediz Graben (İztañ & Yazman 1990; Cohen *et al.* 1995; Emre 1996; Yazman *et al.* 1998; Koçyiğit *et al.* 1999; Yılmaz *et al.* 2000; Sözbilir 2001, 2002; Seyitoğlu *et al.* 2002; Purvis & Robertson 2005a,b), recent studies document that the Miocene deposition is continuous and the Alaşehir and Çaltılık Formations show a gradual contact (Çiftçi & Bozkurt 2009). We parametrically resampled (via Monte Carlo simulation, an option in Paleomagnetism.org for adding published sites for which only the means and Fisher parameters are available) the published data of the Zeytinçayı section. The result shows that this area underwent a counterclockwise rotation of $25 \pm 3.5^\circ$ since deposition of the rocks (Fig. 11a), and provides evidence that there is no differential rotation during the early–middle Miocene transition (Şen & Seyitoğlu 2009).

The Büyük Menderes Graben.

The Eycelli section of Şen & Seyitoğlu (2009) is situated some 5 km north of Nazilli, at the northern border of the Büyük Menderes Graben (Figs 1b and 11a). The sampling spans the early Miocene Hasköy Formation and the middle Miocene Gökkırantepe Formation (Fig. 3). The Hasköy Formation is characterized by fluvio-lacustrine clays, silts and sandstones with a few interlayered lignite horizons, whereas the Gökkırantepe Formation consists of pinkish to red mudstones, sandstones and conglomerates. There is some controversy about the exact age of Büyük Menderes Graben units (Sözbilir & Emre 1990; Cohen *et al.* 1995; Bozkurt 2000; Güner *et al.* 2001, 2009; Şen & Seyitoğlu 2009), but according to Koçyiğit (2015), Miocene deposition along the graben was uninterrupted. Along the Eycelli section, Şen & Seyitoğlu (2009) analysed 52 samples including the contact between the Hasköy and Gökkırantepe Formations. We parametrically resampled their published results, which show that the area underwent a clockwise

rotation of $33 \pm 6^\circ$. As in the Gediz Graben, no differential rotation has been recognized during the early to middle Miocene transition in the Büyük Menderes Graben. Şen & Seyitoğlu (2009) considered that the opposite rotations of the Zeytinçayı ($25 \pm 3.5^\circ$ CCW) and Eycelli ($33 \pm 6^\circ$ CW) sections (Fig. 11a) may have been caused by local tectonics and may be the result of extensional deformation characterized by detachment faults that gave way to the Gediz and Büyük Menderes Graben.

Chios.

Kondopoulou *et al.* (2011) published some results from early–middle Miocene (mammal zone MN5) sedimentary units, which correspond approximately to the lower sequence (Figs 1b and 3). They documented a CCW rotation of $12 \pm 5^\circ$ by combining all normal and reversed polarity data (Fig. 11a). However, a reversal test is not reported (mean normal and reversed directions are not given separately), but glancing at their plots the test is most probably negative. Kondopoulou *et al.* explained these anomalous directions by suggesting that Chios is most probably affected by the strike-slip tectonism of the İzmir–Balıkesir Transfer Zone.

The İzmir–Balıkesir Transfer Zone as a link between Cycladic and west Anatolian basins.

Uzel *et al.* (2015) analysed more than a thousand samples at 96 localities distributed within the İzmir–Balıkesir Transfer Zone and graben basins (Fig. 1b). The drilling locations were concentrated not only in the Miocene volcano-sedimentary units, but also in the syn-extensional granites intruded into the Menderes Core Complex during its exhumation (Fig. 11a). Uzel *et al.* identified two rotational phases belonging to two different stratigraphical sequences during the Miocene: (1) an early Miocene phase; (2) a middle–late Miocene phase. For the early Miocene, they

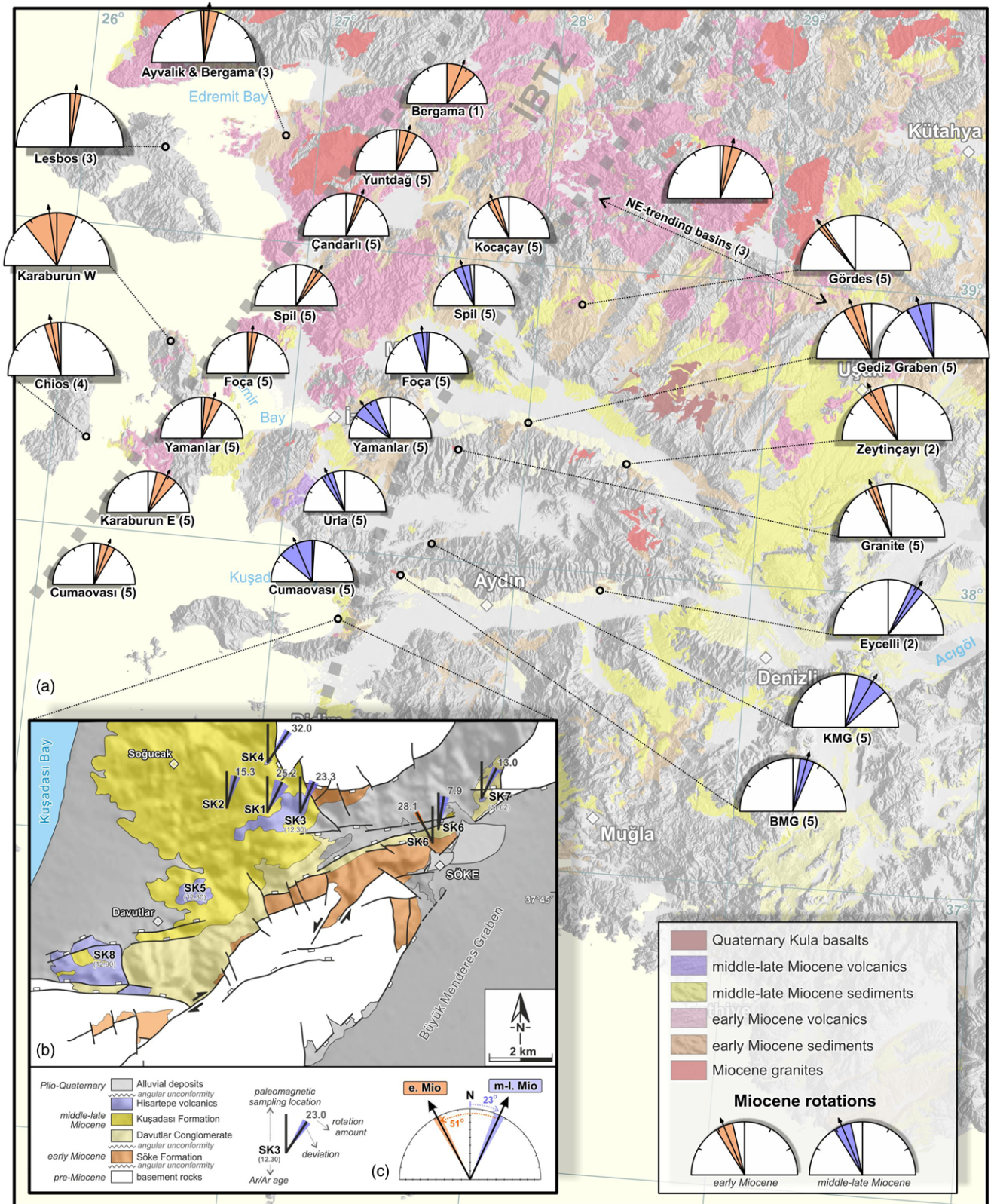


Fig. 11. (a) Palaeomagnetic data from previous palaeomagnetic studies (modified from Uzel *et al.* 2015) draped onto simplified geological map of western Anatolia (GDMRE 2002). Data sources: (1) Kissel *et al.* (1987); (2) Şen & Seyitoğlu (2009); (3) van Hinsbergen *et al.* (2010a); (4) Kaymakci *et al.* (2007); (5) Uzel *et al.* (2015). (b) Geological map showing the distribution of palaeomagnetic rotations and the $^{40}\text{Ar}/^{39}\text{Ar}$ ages from the Söke Basin. It should be noted that the rotational differentiation between lower and upper part of middle Miocene unconformity is about 51° . Please see online version for colour.

speculated that the clockwise rotations reflect the main rotations within the İzmir–Balıkesir Transfer Zone (*c.* 31° CW), whereas the area outside this zone, covering the Gediz, Küçük Menderes and Büyük Menderes Grabens, consistently experienced on

average a counterclockwise rotation (*c.* 23° CCW). Like the volcano-sedimentary rocks, the early Miocene syn-extensional granites in the graben area also recorded a counterclockwise rotation (*c.* 22° CCW). For the middle-late Miocene sequences

above the middle Miocene unconformity Uzel *et al.* identified a tectonic reorganization in terms of rotations. At this time, the stratigraphy within the İzmir–Balıkesir Transfer Zone area recorded counterclockwise rotation (*c.* 23° CCW), whereas the graben area showed a clockwise rotation (*c.* 25° CW). Along the Mid-Cycladic Lineament, these opposite senses in rotation were also recognized in the Greek Islands (Walcott & White 1998). For example, whereas the middle Miocene granites in the western part of the structure rotated clockwise (23° CW, on Tinos and Mykonos), the same granites in the eastern part of the Mid-Cycladic Lineament experienced counterclockwise (*c.* 30° CCW, on Naxos) rotations.

Our palaeomagnetic results presented here also support two distinct rotational phases for the Miocene (Fig. 11) and agree well with the rotational reorganization mechanism along the İzmir–Balıkesir Transfer Zone as reported by Uzel *et al.* (2015). The early Miocene sedimentary rocks below the middle Miocene unconformity show on average a counterclockwise rotation (*c.* 51° = 28° CCW + 23° CW) between the early Miocene and the middle–late Miocene, whereas the middle–late Miocene volcano-sedimentary rocks lying above the middle Miocene unconformity recorded an average clockwise rotation (*c.* 23°). Moreover, CW (*c.* 18°) rotation data of Uzel *et al.* (2015) from the Balatçık volcanic series located just NE of the Söke Basin are also coherent with this second rotational phase of the region (Fig. 11).

Tectonic implications for the Aegean region

Recent studies such as those by Beniést *et al.* (2016) and Brun *et al.* (2016) suggested that the two-stage extension of Neogene basins at the whole Aegean scale attests to a major tectonic change owing to an acceleration of the slab roll-back–tear process in the middle Miocene. The subduction roll-back process also plays an important role in the initiation and development of back-arc extensional basins, in particular when the velocity of subduction roll-back exceeds the velocity of plate convergence (Dewey 1980; Hale *et al.* 2010). Indeed, in the Söke Basin, two similar sedimentary packages, each related to basin formation during extensional phases, are separated from each other by a notable angular unconformity during the middle Miocene. We conclude that this unconformity is therefore most probably associated with an important event that took place in the Aegean region. Here, the roll-back process had been triggered by tearing of the slab, increasing the velocity of upper crustal fragmentation, thus allowing the formation of basins that are controlled by high-angle normal faults. In addition, the regional rotation data of Uzel *et al.* (2015), combined with the results of Çiftçi & Bozkurt (2009) and Şen & Seyitoğlu (2009), showing that Miocene deposition within the graben basins is continuous, suggest that this separation is effective only within the İzmir–Balıkesir Transfer Zone, highlighted by a major angular unconformity and opposite rotational behaviour. Hence, we conclude that a difference in the magnitude of extension is most probably the cause of the tectonic reorganization of the İzmir–Balıkesir Transfer Zone reported by Uzel *et al.* (2015), rather than a period of compression. The direction of extension was changing between NNE and NW during the Miocene time interval, according to regional kinematic studies on the İzmir–Balıkesir Transfer Zone (Özkaymak *et al.* 2013; Sümer *et al.* 2013; Uzel *et al.* 2013).

The dynamics of this slab tearing process in the Aegean region have also been discussed in several studies (e.g. de Boorder *et al.* 1998; Wortel & Spakman 2000; Govers & Wortel 2005; van Hinsbergen *et al.* 2005b, 2010b; Biryol *et al.* 2011). Jolivet *et al.* (2013) reported that the Aegean slab retreat proceeds by acquiring strong curvature geometry and a lateral tearing below the Aegean crust. This tearing event affected the geological surface expression

in the middle Miocene and alkaline volcanism started in the region as a result of the penetration of the asthenospheric flows, such as the NE–SW-trending volcanism along the İzmir–Balıkesir Transfer Zone (Kaya 1981; Uzel & Sözbilir 2008). Jolivet *et al.* (2015) also pointed out that a high-temperature anomaly in the crust, which requires a similar anomaly in the mantle, has migrated at a fast pace by using this torn gap during the middle Miocene. Therefore in western Anatolia, the lateral variation of extension must be compensated by the development of an accommodation zone, such as the İzmir–Balıkesir Transfer Zone. Gessner *et al.* (2013) proposed that this discontinuity is a part of a lithospheric-scale shear zone, which has been accommodated in the Aegean and the Anatolian regions, and suggested that the İzmir–Balıkesir Transfer Zone is a surface expression of this slab-tear since the Miocene.

In addition, the reorganization of the inferred rotation phases for the Söke Basin during the middle Miocene shows a remarkable coincidence with some tectonic changes in western Anatolia. After the southward and CCW movement of the Lycian Nappes above the Menderes core complex, the exhumation of metamorphic rocks occurred contemporaneously (Hayward & Robertson 1982; Hayward 1984; Collins & Robertson 1998, 2003; Sözbilir 2005). Geological evidence indicates that the tectonic denudation of the Menderes core complex occurred in at least two stages (Ring *et al.* 2003; Purvis & Robertson 2004; Bozkurt *et al.* 2011; Hetzel *et al.* 2013). First, with movement on the Simav detachment and Büyük Menderes shear zone, the northern and southern part of the Menderes Massif were exhumed during the interval 19–16 Ma (Ring & Collins 2005; Thomson & Ring 2006; Gessner *et al.* 2013; Hetzel *et al.* 2013), contemporaneous with the syn-extensional granites (Catlos *et al.* 2011, 2012). The first appearance of metamorphic clasts in western Anatolian basins is also dated as early Miocene (Sözbilir 2005), which means that the metamorphic rocks are on the surface in this period. In the next stage, the central part of the massif was exhumed along the Gediz and Büyük Menderes detachment faults between 12 and 3 Ma (Bozkurt *et al.* 2011; Hetzel *et al.* 2013). Moreover, based on available fission-track data, a break in exhumation and change in deformation across the Menderes core complex took place during the middle Miocene (Gessner *et al.* 2001, 2013; Ring *et al.* 2003; Thomson & Ring 2006; Brun *et al.* 2016). Either the two phases of denudation–extension were separated by a short period of dominantly compression, or alternatively the amount of extension has changed.

Conclusions

To obtain quantitative constraints on the middle Miocene unconformity observed within the Söke Basin, ⁴⁰Ar/³⁹Ar radioisotope and palaeomagnetic analyses have been performed. The main findings of the present study are as follows.

- (1) The basin contains a number of intra-continental alkaline volcanic bodies formed along the localized shear zone. The exact timing of rotational events in these volcanic bodies has been derived from ⁴⁰Ar/³⁹Ar dating. According to the geochronological results, volcanic activity occurred near-synchronously in the Söke region, ranging between 11.66 and 12.85 Ma, indicating a *c.* 1.2 myr episode. This provides an upper limit for the duration of the middle Miocene unconformity and the timing of rotation of volcano-sedimentary rocks after this interruption.
- (2) Our rotation data indicate that the Söke Basin has in total experienced a 51 ± 5° counterclockwise rotation during the time represented by the middle Miocene unconformity. After the middle Miocene, the rotation direction was reversed, and the basin has experienced a 23 ± 5° clockwise rotation since the Pliocene.

- (3) The main driver for the rotations of the Söke Basin must have been the İzmir–Balıkesir Transfer Zone as an inherited structure transferring the regional extension between the Cycladic and Menderes core complexes. Most probably, this gave way to the change in the rotation senses that occurred along the eastern margin of the İzmir–Balıkesir Transfer Zone and is directly related to the reorganization in the movement of this zone itself.
- (4) According to available fission-track and age data, the timing of the middle Miocene unconformity falls within the period between two separate phases of exhumation of the Menderes core complex in western Anatolia. We suggest that a change in the magnitude and direction of extension owing to the acceleration of trench retreat has most probably caused the reverse rotation senses in the region.

Acknowledgements We thank M. Dekkers, T. Mullender, P. Ertepinar and M. Meijers for collaboration and critical comments on the palaeomagnetic measurements; and J. Wijbrans & R. van Elsas for their help during the dating analyses. We also thank the editor C. Mac Niocaill and two anonymous reviewers for their constructive comments, which greatly improved the paper.

Funding This work is a part of the PhD study of B.U. and is supported by the Scientific and Technical Research Council of Turkey (TÜBİTAK) research grant of ÇAYDAĞ-109Y044 and partly by the Dokuz Eylül University Scientific Research (BAP) Project of 2007.KB.FEN.039.

Scientific editing by Conall Mac Niocaill

References

- Akgün, F. & Akyol, E. 1999. Palynostratigraphy of the coal bearing Neogene deposits graben in Büyük Menderes Western Anatolia. *Geobios*, **32**, 367–383.
- Avigad, D., Baer, G. & Heimann, A. 1998. Block rotations and continental extension in central Aegean Sea: Palaeomagnetic and structural evidence from Tinos and Mykonos (Cyclades, Greece). *Earth and Planetary Science Letters*, **157**, 23–40.
- Beccaletto, L. & Steiner, C. 2005. Evidence of two-stage extensional tectonics from the northern edge of the Edremit Graben (NW Turkey). *Geodinamica Acta*, **18**, 283–297.
- Becker-Platen, J.D. 1970. *Lithostratigraphische Untersuchungen in Kanozoikum Südwest Anatoliens (Türkei) (Kanozoikum und Braunkohlen der Türkei)*. Beihefte zum Geologischen Jahrbuch, **97**.
- Beniest, A., Brun, J.P., Gorini, C., Crombez, V., Deschamps, R., Hamon, Y. & Smit, J. 2016. Interaction between trench retreat and Anatolian escape as recorded by Neogene basins in the northern Aegean Sea. *Marine and Petroleum Geology*, **77**, 30–42.
- Besenecker, H. 1973. *Neogen und Quartär der Insel Chios (Ägäis)*. PhD thesis, Freien Universität Berlin.
- Biggin, A.J., Strik, G.H.M.A. & Langereis, C.G. 2008a. Evidence for a very long-term trend in geomagnetic secular variation. *Nature Geoscience*, **1**, 395–398.
- Biggin, A., van Hinsbergen, D.J.J., Langereis, C.G., Straathof, G.B. & Deenen, M.H. 2008b. Geomagnetic secular variation in the Cretaceous Normal Superchron and in the Jurassic. *Physics of the Earth and Planetary Interiors*, **169**, 3–19.
- Biryol, C.B., Beck, S.L., Zandt, G. & Özacar, A.A. 2011. Segmented African lithosphere beneath the Anatolian region inferred from teleseismic P-wave tomography. *Geophysical Journal International*, **184**, 1037–1057.
- Bozkurt, E. 2000. Timing of extension on the Büyük Menderes Graben, western Turkey, and its tectonic implications. In: Bozkurt, E., Winchester, J.A. & Piper, J.D.A. (eds) *Tectonics and Magmatism in Turkey and the Surrounding Area*. Geological Society, London, Special Publications, **173**, 385–403, <https://doi.org/10.1144/GSL.SP.2000.173.01.18>
- Bozkurt, E. 2001a. Late Alpine evolution of the central Menderes Massif, western Anatolia, Turkey. *International Journal of Earth Sciences*, **89**, 728–744.
- Bozkurt, E. 2001b. Neotectonics of Turkey—a synthesis. *Geodinamica Acta*, **14**, 3–30.
- Bozkurt, E. & Mittweide, S.K. 2005. Introduction: evolution of Neogene extensional tectonics of western Turkey. *Geodinamica Acta*, **18**, 153–165.
- Bozkurt, E. & Sözbilir, H. 2004. Tectonic evolution of the Gediz Graben: field evidence for an episodic, two-stage extension in western Turkey. *Geological Magazine*, **141**, 63–79.
- Bozkurt, E. & Sözbilir, H. 2006. Evolution of the large-scale active Manisa Fault, southwest Turkey: Implications on fault development and regional tectonics. *Geodinamica Acta*, **19**, 427–453.
- Bozkurt, E., Satir, M. & Buğdaycıoğlu, Ç. 2011. Surprisingly young Rb/Sr ages from the Simav extensional detachment fault zone, northern Menderes Massif, Turkey. *Journal of Geodynamics*, **52**, 406–431, <https://doi.org/10.1016/j.jog.2011.06.002>
- Bradley, K.E., Vassilakis, E., Hosa, A. & Weiss, B.P. 2013. Segmentation of the Hellenides recorded by Pliocene initiation of clockwise block rotation in Central Greece. *Earth and Planetary Science Letters*, **362**, 6–19.
- Brun, J.P., Faccenna, C., Gueydan, F., Sokoutis, D., Philippon, M., Kydonakis, K. & Gorini, C. 2016. The two-stage Aegean extension, from localized to distributed, a result of slab rollback acceleration. *Canadian Journal of Earth Sciences*, **53**, 1142–1157, <https://doi.org/10.1139/cjes-2015-0203>
- Butler, R.F. 1992. *Paleomagnetism: Magnetic Domains to Geologic Terranes*. Blackwell Scientific, Oxford.
- Çakmaköglü, A. 2007. Dilek Yarımadası, Söke ve Selçuk çevresinin Neojen öncesi tektonostratigrafisi. *Bulletin of Mineral Research and Exploration of Turkey*, **135**, 1–17.
- Candan, O., Dora, O.Ö., Oberhänsli, R., Oelsner, F. & Dürr, S. 1997. Blueschist relics in the Mesozoic cover series of the Menderes Massif and correlations with Samos Island, Cyclades. *Schweizerische Mineralogische und Petrographische Mitteilungen*, **77**, 95–99.
- Çatlos, E.J., Baker, C., Sorensen, S.S., Jacob, L. & Çemen, I. 2011. Linking microcracks and mineral zoning of detachment-exhumed granites to their tectonomagmatic history: Evidence from the Salihli and Turgutlu plutons in western Turkey (Menderes Massif). *Journal of Structural Geology*, **33**, 951–969.
- Çatlos, E.J., Jacobs, L., Oyman, T. & Sorensen, S. 2012. Long-term exhumation of Aegean metamorphic core complex granitoids in the northern Menderes Massif, western Turkey. *American Journal of Science*, **312**, 534–571.
- Çetinkaplan, M. 2002. *Tertiary high pressure/low temperature metamorphism in the Mesozoic cover series of the Menderes Massif and correlation with the Cycladic Crystalline Complex*. PhD thesis, Dokuz Eylül University, İzmir.
- Çiftçi, N.B. & Bozkurt, E. 2009. Evolution of the Miocene sedimentary fill of the Gediz Graben, SW Turkey. *Sedimentary Geology*, **216**, 49–79.
- Çiftçi, G., Pamukçu, O., Çoruh, C., Çopur, S. & Sözbilir, H. 2011. Shallow and deep structure of a supradetachment basin based on geological, conventional deep seismic reflection sections and gravity data in the Büyük Menderes Graben, western Anatolia. *Surveys in Geophysics*, **32**, 271–290.
- Çinku, M.C., Hisarlı, M. et al. 2015. Evidence of Late Cretaceous oroclinal bending in north–central Anatolia: palaeomagnetic results from Mesozoic and Cenozoic rocks along the İzmir–Ankara–Erzincan Suture Zone. In: Pueyo, E. L., Cifelli, F., Sussman, A.J. & Oliva-Urcia, B. (eds) *Palaeomagnetism in Fold and Thrust Belts: New Perspectives*. Geological Society, London, Special Publications, **425**, Dokuz Eylül University, İzmir.
- Cohen, H.A., Dart, C.J., Akyüz, H.S. & Barka, A. 1995. Syn-rift sedimentation and structural development of the Gediz and Büyük Menderes graben, western Turkey. *Journal of the Geological Society, London*, **152**, 629–638, <https://doi.org/10.1144/gsjgs.152.4.0629>
- Collins, A.S. & Robertson, A.H.F. 1998. Processes of Late Cretaceous to Late Miocene episodic thrust sheet translation in the Lycian Taurides, SW Turkey. *Journal of the Geological Society, London*, **155**, 759–772, <https://doi.org/10.1144/gsjgs.155.5.0759>
- Collins, A.S. & Robertson, A.H.F. 2003. Kinematic evidence for late Mesozoic–Miocene emplacement of the Lycian Allochthon over the Western Anatolia Belt, SW Turkey. *Geological Journal*, **38**, 1–16.
- Dadd, K.A. & van Wagoner, N.A. 2002. Magma composition and viscosity as controls on peperite texture: an example from Passamaquoddy Bay, southeastern Canada. *Journal of Volcanology and Geothermal Research*, **114**, 63–80.
- De Boorder, H., Spakman, W., White, S.H. & Wortel, M.J.R. 1998. Late Cenozoic mineralization, orogenic collapse and slab detachment in the European Alpine Belt. *Earth and Planetary Science Letters*, **164**, 569–575.
- Deenen, M.H.L., Langereis, C.G., van Hinsbergen, D.J.J. & Biggin, A.J. 2011. Geomagnetic secular variation and the statistics of palaeomagnetic directions. *Geophysical Journal International*, **186**, 509–520.
- Deenen, M.H.L., Langereis, C.G., Van Hinsbergen, D.J.J. & Biggin, A.J. 2014. Erratum to Geomagnetic secular variation and the statistics of palaeomagnetic directions [Geophysical Journal International, 186, (2011) 509–520]. *Geophysical Journal International*, **197**, 643.
- Dewey, J.F. 1980. Episodicity, sequence, and style at convergent plate boundaries. In: Strangway, D.W. (ed.) *The Continental Crust And Its Mineral Deposits*. Geological Association of Canada Special Paper, **20**, 553–573.
- Dewey, J.F., Hempton, M.R., Kidd, W.S.F., Şaroğlu, F. & Şengör, A.M.C. 1986. Shortening of continental lithosphere: the neotectonics of eastern Anatolia—a young collision zone. In: Coward, M.P. & Ries, A.C. (eds) *Collision Tectonics*. Geological Society, London, Special Publications, **19**, 3–37, <https://doi.org/10.1144/GSL.SP.1986.019.01.01>
- Dora, O.Ö., Candan, O., Kaya, O., Koralay, E. & Dürr, S. 2001. Revision of the so-called ‘leptite–gneisses’ in the Menderes Massif: a supracrustal metasedimentary origin. *International Journal of Earth Science*, **89**, 836–851.
- Dosseto, A., Turner, S. & Van-Orma, J. 2011. *Timescales of Magmatic Processes*. Wiley, New York.
- Duermeijer, C.E., Krijgsman, W., Langereis, C.G. & Ten Veen, J.H. 1998. Post-early Messinian counterclockwise rotations on Crete: implications for Late Miocene to Recent kinematics of the southern Hellenic arc. *Tectonophysics*, **298**, 177–189.
- Duermeijer, C.E., Nyst, M., Meijer, P.T., Langereis, C.G. & Spakman, W. 2000. Neogene evolution of the Aegean arc: palaeomagnetic and geodetic evidence

- for a rapid and young rotation phase. *Earth and Planetary Science Letters*, **176**, 509–525.
- Ediger, V., Batu, Z. & Yazman, M. 1996. Paleopalynology of possible hydrocarbon source rocks of the Alaşehir–Turgutlu area in the Gediz graben (western Anatolia). *Turkish Association of Petroleum Geologists Bulletin*, **8**, 94–112.
- Emre, T. 1996. Geology and tectonics of the Gediz Graben. *Turkish Journal of Earth Sciences*, **5**, 171–185.
- Emre, T. & Sözbilir, H. 2007. Tectonic evolution of the Kiraz Basin, Küçük Menderes Graben: evidence for compression/uplift-related basin formation overprinted by extensional tectonics in West Anatolia. *Turkish Journal of Earth Sciences*, **16**, 441–470.
- Ercan, T., Akat, U., Günay, E. & Savaşçın, Y. 1986. Geology of the area around Söke–Selçuk–Kuşadası and petrochemical characteristics of volcanic rocks. *Bulletin of Mineral Research and Exploration of Turkey*, **105–106**, 15–38.
- Fisher, R.A. 1953. Dispersion on a sphere. *Proceedings of the Royal Society of London, Series A*, **217**, 295–305. <https://doi.org/10.1098/rspa.1953.0064>
- Forster, M. & Lister, G. 2009. Core-complex-related extension of the Aegean lithosphere initiated at the Eocene–Oligocene transition. *Journal of Geophysical Research*, **114**, B02401. <https://doi.org/10.1029/2007JB005382>
- Gautier, P., Brun, J.P., Moriceau, R., Sokoutis, D., Martinod, J. & Jolivet, L. 1999. Timing, kinematics and cause of the Aegean extension: A scenario based on a comparison with simple analogues experiments. *Tectonophysics*, **315**, 31–72.
- GDMRE 2002. *Geological Map of Turkey, 1/500.000 scale*. General Directorate of Mineral Research and Exploration, Ankara, 7–8.
- Gessner, K., Piazzolo, S., Güngör, T., Ring, U., Kroner, A. & Passchier, C.W. 2001. Tectonic significance of deformation patterns in granitoid rocks of the Menderes nappes, Anatolide belt, southwest Turkey. *International Journal of Earth Sciences*, **89**, 766–780.
- Gessner, K., Gallardo, L.A., Markwitz, V., Ring, U. & Thomson, S.N. 2013. What caused the denudation of the Menderes Massif: Review of crustal evolution, lithosphere structure, and dynamic topography in southwest Turkey. *Gondwana Research*, **24**, 243–274.
- Glodny, J. & Hetzel, R. 2007. Precise U–Pb ages of syn-extensional Miocene intrusions in the central Menderes Massif, Western Turkey. *Geological Magazine*, **144**, 235–246.
- Govers, R. & Wortel, M.J.R. 2005. Lithosphere tearing at STEP faults: response to edges of subduction zones. *Earth and Planetary Science Letters*, **236**, 505–523.
- Gülüzyü, E., Kaymakçı, N. et al. 2013. Late Eocene evolution of the Çiçekdağı Basin (central Turkey): Syn-sedimentary compression during microcontinent–continent collision in central Anatolia. *Tectonophysics*, **602**, 286–299.
- Gürer, F.Ö., Bozcu, M., Yılmaz, K. & Yılmaz, Y. 2001. Neogene basin development around Söke–Kuşadası (western Anatolia) and its bearing on tectonic development of the Aegean region. *Geodinamica Acta*, **14**, 57–69.
- Gürer, F.Ö., Sarıca-Filoreau, N., Özbüran, M., Sangu, E. & Doğan, B. 2009. Progressive development of the Büyük Menderes Graben based on new data, western Turkey. *Geological Magazine*, **146**, 652–673.
- Gürsoy, H., Piper, J.D.A., Tatar, O. & Temiz, H. 1997. A palaeomagnetic study of the Sivas Basin, Central Turkey: crustal deformation during lateral extrusion of the Anatolian Block. *Tectonophysics*, **271**, 89–105.
- Gürsoy, H., Piper, J.D.A., Tatar, O. & Mesci, L. 1998. Palaeomagnetic study of the Karaman and Karapınar volcanic complexes, central Turkey: neotectonic rotation in the south–central sector of the Anatolian Block. *Tectonophysics*, **299**, 191–211.
- Gürsoy, H., Piper, J.D.A. & Tatar, O. 1999. Palaeomagnetic study of the Galatean Volcanic Province, north–central Turkey: Neogene deformation at the northern border of the Anatolian Block. *Geological Journal*, **34**, 7–23.
- Gürsoy, H., Piper, J.D.A. & Tatar, O. 2003. Neotectonic deformation in the western sector of tectonic escape in Anatolia: Palaeomagnetic study of the Afyon region, central Turkey. *Tectonophysics*, **374**, 57–79.
- Hale, A.J., Gottschald, K.D., Rosenbaum, G., Bourgoign, L., Bauchy, M. & Münhahaus, H. 2010. Dynamics of slab tear faults: insights from numerical modelling. *Tectonophysics*, **483**, 58–70.
- Hayward, A.B. 1984. Sedimentation and basin formation related to ophiolite nappe emplacement, Miocene, SW Turkey. *Sedimentary Geology*, **71**, 105–129.
- Hayward, A.B. & Robertson, A.H.F. 1982. Direction of ophiolite emplacement inferred from Cretaceous and Tertiary sediments of an adjacent autochthon, the Bey Dağları, southwest Turkey. *Geological Society of America Bulletin*, **93**, 68–75.
- Hetzel, R., Zwingmann, H. et al. 2013. Spatio-temporal evolution of brittle normal faulting and fluid infiltration in detachment fault systems—a case study from the Menderes Massif, western Turkey. *Tectonics*, **32**, 364–376.
- Hilgen, F.J., Lourens, L.J. et al. 2012. The Neogene Period. In: Gradstein, F.M., Ogg, J.G., Schmitz, M.D. & Ogg, G.M. (eds) *The Geologic Time Scale*. Elsevier, Boston, MA, 923–978.
- İşseven, T. & Tüysüz, O. 2006. Palaeomagnetically defined rotations of fault-bounded continental blocks in the North Anatolian Shear Zone, North Central Anatolia. *Journal of Asian Earth Sciences*, **28**, 469–479.
- İzitan, H. & Yazman, M. 1990. Geology and hydrocarbon potential of the Alaşehir (Manisa) area, western Turkey. In: Savaşçın, M.Y. & Eronat, A.H. (eds) *Proceedings of International Earth Sciences Congress on Aegean Regions*, İzmir, **1**, 327–338.
- Jolivet, L. & Brun, J.P. 2010. Cenozoic geodynamic evolution of the Aegean. *International Journal of Earth Sciences*, **99**, 109–138.
- Jolivet, L., Faccenna, C. et al. 2013. Aegean tectonics: Strain localisation, slab tearing and trench retreat. *Tectonophysics*, **597–598**, 1–33.
- Jolivet, L., Menant, A. et al. 2015. The geological signature of a slab tear below the Aegean. *Tectonophysics*, **659**, 166–182.
- Kaya, O. 1981. Miocene reference section for the coastal parts of West Anatolia. *Newsletters on Stratigraphy*, **10**, 164–191.
- Kaya, O., Ünay, G., Eichhorn, S., Hassenrück, S., Knappe, A. & Pekdeğer, A. 2004. Halitpaşa Transpressive Zone: Implications for an Early Pliocene compressional phase in central western Anatolia, Turkey. *Turkish Journal of Earth Sciences*, **13**, 1–13.
- Kaya, O., Ünay, E., Göktaş, F. & Saraç, G. 2007. Early Miocene stratigraphy of Central West Anatolia, Turkey: implications for the tectonic evolution of the Eastern Aegean area. *Geological Journal*, **42**, 85–109.
- Kaymakçı, N. 2006. Kinematic development and paleostress analysis of Denizli Basin (W Turkey): implications of spatial variation of relative paleostress magnitudes and orientations. *Journal of Asian Earth Science*, **27**, 207–222.
- Kaymakçı, N., White, S.H. & van Dijk, P.M. 2003. Kinematic and structural development of the Çankırı Basin (Central Anatolia, Turkey): a palaeostress inversion study. *Tectonophysics*, **364**, 85–113.
- Kaymakçı, N., Aldanmaz, E., Langereis, C., Spell, T.L., Gurer, O.F. & Zanetti, K. A. 2007. Late Miocene transcurent tectonics in NW Turkey: evidence from palaeomagnetism and ⁴⁰Ar–³⁹Ar dating of alkaline volcanic rocks. *Geological Magazine*, **144**, 379–392.
- Kirschvink, J.L. 1980. The least-squares line and plane and the analysis of palaeomagnetic data. *Geophysical Journal of the Royal Astronomical Society*, **62**, 699–718.
- Kissel, C., Laj, C., Poisson, A., Savaşçın, Y., Simeakis, K. & Mercier, J.L. 1986. Palaeomagnetic evidence for Neogene rotational deformations in the Aegean domain. *Tectonics*, **5**, 783–795.
- Kissel, C., Laj, C., Şengör, A.M.C. & Poisson, A. 1987. Palaeomagnetic evidence for rotation in opposite senses of adjacent blocks in northeastern Aegean and Western Anatolia. *Geophysical Research Letters*, **14**, 907–910.
- Kissel, C., Averbuch, O., Frizon de Lamotte, D., Monod, O. & Allerton, S. 1993. First palaeomagnetic evidence for a post-Eocene clockwise rotation of the Western Taurides thrust belt east of the Isparta reentrant (Southwestern Turkey). *Earth and Planetary Science Letters*, **117**, 1–14.
- Kissel, C., Laj, C., Poisson, A. & Görür, N. 2002. Palaeomagnetic reconstruction of the Cenozoic evolution of the Eastern Mediterranean. *Tectonophysics*, **362**, 199–217.
- Koçyiğit, A. 2005. The Denizli graben–horst system and the eastern limit of western Anatolian continental extension: basin fill, structure, deformational mode, throw amount and episodic evolutionary history, SW Turkey. *Geodinamica Acta*, **18**, 167–128.
- Koçyiğit, A. 2015. An overview on the main stratigraphic and structural features of a geothermal area: the case of Nazilli–Buharkent section of the Büyük Menderes Graben, SW Turkey. *Geodinamica Acta*, **27**, 1–25.
- Koçyiğit, A. & Deveci, S. 2007. A N–S-trending active extensional structure, the Suhut (Afyon) graben: Commencement age of the extensional neotectonic period in the Isparta Angle, SW Turkey. *Turkish Journal of Earth Sciences*, **16**, 391–416.
- Koçyiğit, A. & Özçaçar, A.A. 2003. Extensional neotectonic regime through the NE edge of the Outer Isparta Angle, SW Turkey: new field and seismic data. *Turkish Journal of Earth Sciences*, **12**, 67–90.
- Koçyiğit, A., Yusufoglu, H. & Bozkurt, E. 1999. Evidence from the Gediz Graben for episodic two-stage extension in western Turkey. *Journal of the Geological Society, London*, **156**, 605–616. <https://doi.org/10.1144/gsjgs.156.3.0605>
- Kondopoulou, D. 2000. Palaeomagnetism in Greece: Cenozoic and Mesozoic components and their geodynamic implications. *Tectonophysics*, **326**, 151–151.
- Kondopoulou, D., Şen, Ş., Aidona, E., van Hinsbergen, D.J.J. & Koufos, G. 2011. Rotation history of Chios Island, Greece since the Middle Miocene. *Journal of Geodynamics*, **51**, 327–338.
- Koppers, A.A.P. 2002. ArArCALC-software for ⁴⁰Ar/³⁹Ar age calculations. *Computers and Geosciences*, **28**, 605–619.
- Koufos, G.D., de Bonis, L. & Şen, Ş. 1995. *Lophocyon paraskevaidisi*, a new viverrid (Carnivora, Mammalia) from the Middle Miocene of Chios Island, Greece. *Geobios*, **28**, 511–523.
- Koymans, M.R., Langereis, C.G., Pastor-Galan, D. & van Hinsbergen, D.J.J. 2016. Paleomagnetism.org: an online multi-platform open source environment for paleomagnetic data analysis. *Computers and Geosciences*, **93**, 127–137.
- Kuiper, K.F., Deino, A., Hilgen, F.J., Krijgsman, W., Renne, P.R. & Wijbrans, J. R. 2008. Synchronizing rock clocks of Earth history. *Science*, **320**, 500–504.
- Lefebvre, C.J.C., Meijers, M.J.M., Kaymakçı, N., Peynircioğlu, A.A., Langereis, C.G. & van Hinsbergen, D.J.J. 2013. Reconstructing the geometry of central Anatolia during the late Cretaceous: Large-scale Cenozoic rotations and deformation between the Pontides and Taurides. *Earth and Planetary Science Letters*, **366**, 83–98.
- Le Pichon, X. & Angelier, J. 1979. The Hellenic arc and trench system: A key to the neotectonic evolution of the eastern Mediterranean area. *Tectonophysics*, **60**, 1–42.
- Lindsay, E. 1997. Eurasian mammal biochronology: An overview. *Palaeogeography, Palaeoclimatology, Palaeoecology*, **133**, 117–128.

- Meijers, M.J.M., Kaymakçı, N., van Hinsbergen, D.J.J., Langereis, C.G., Stephenson, R.A. & Hippolyte, J.C. 2010. Late Cretaceous to Paleocene oroclinal bending in the Central Pontides (Turkey). *Tectonics*, **45**, 7–39.
- Meijers, M.J.M., Van Hinsbergen, D.J.J., Dekkers, M.J., Altiner, D., Kaymakçı, N. & Langereis, C.G. 2011. Pervasive Palaeogene remagnetization of the central Taurides fold-and-thrust belt (southern Turkey) and implications for rotations in the Isparta Angle. *Geophysical Journal International*, **184**, 1090–1112.
- Meulenkamp, J.E., Wortel, M.J.R., van Wamel, W.A., Spakman, W. & Hoogerduyn, S.E. 1988. On the Hellenic subduction zone and the geodynamical evolution of Crete since the late middle Miocene. *Tectonophysics*, **146**, 203–215.
- Min, K., Mundil, R., Renne, P.R. & Ludwig, K.R. 2000. A test for systematic errors in $^{40}\text{Ar}/^{39}\text{Ar}$ geochronology through comparison with U/Pb analysis of a 1.1-Ga rhyolite. *Geochimica et Cosmochimica Acta*, **64**, 73–98.
- Morris, A. & Anderson, M. 1996. First palaeomagnetic results from the Cycladic Massif, Greece, and their implications for Miocene extension directions and tectonic models in the Aegean. *Earth and Planetary Science Letters*, **142**, 397–408.
- Mullender, T.A.T., van Velzen, A.J. & Dekkers, M.J. 1993. Continuous drift correction and separate identification of ferrimagnetic and paramagnetic contribution in thermomagnetic runs. *Geophysical Journal International*, **114**, 663–672.
- Nier, A.O. 1950. A redetermination of the relative abundances of the isotopes of carbon, nitrogen, oxygen, argon, and potassium. *Physical Review*, **77**, 789–793.
- Oberhänsli, R., Monie, P. & Candan, O. 1998. The age of blueschist metamorphism in the Mesozoic cover series of the Menderes Massif. *Schweizerische Mineralogische und Petrographische Mitteilungen*, **78**, 309–316.
- Okay, A.İ. 2001. Stratigraphic and metamorphic inversions in the central Menderes Massif: a new structural model. *International Journal of Earth Science*, **89**, 709–727.
- Özkaymak, Ç., Sözbilir, H. & Uzel, B. 2013. Neogene–Quaternary evolution of the Manisa Basin: evidence for variation in the stress pattern of the Izmir–Balıkesir Transfer Zone, western Anatolia. *Journal of Geodynamics*, **65**, 117–135.
- Pe-Piper, G., Piper, D.J.W. & Matarangas, D. 2002. Regional implications of geochemistry and style of emplacement of Miocene I-type diorite and granite, Delos, Cyclades, Greece. *Lithos*, **60**, 47–66.
- Philippon, M., Brun, J.P. & Gueydan, F. 2012. Deciphering subduction from exhumation in the segmented Cycladic Blueschist Unit (Central Aegean, Greece). *Tectonophysics*, **524–525**, 116–134.
- Philippon, M., Brun, J.P., Gueydan, F. & Sokoutis, D. 2014. The interaction between Aegean back-arc extension and Anatolia escape since Middle Miocene. *Tectonophysics*, **631**, 176–188.
- Piper, J.D.A., Moore, J., Tatar, O., Gürsoy, H. & Park, R.G. 1996. Palaeomagnetic study of crustal deformation across an intracontinental transform: the North Anatolian Fault Zone in Northern Turkey. In: Morris, A. & Tarling, D.H. (eds) *Paleomagnetism of the Mediterranean Regions*. Geological Society, London, Special Publications, **105**, 299–310, <https://doi.org/10.1144/GSL.SP.1996.105.01.26>
- Piper, J.D.A., Tatar, O. & Gürsoy, H. 1997. Deformational behaviour of continental lithosphere deduced from block rotations across the North Anatolian Fault Zone in Turkey. *Earth and Planetary Science Letters*, **150**, 191–203.
- Piper, J.D.A., Gürsoy, H. & Tatar, O. 2002. Palaeomagnetism and magnetic properties of the Cappadocian ignimbrite succession, central Turkey and Neogene tectonics of the Anatolian collage. *Journal of Volcanology and Geothermal Research*, **117**, 237–262.
- Piper, J.D.A., Tatar, O., Gürsoy, H., Kocbulut, F. & Mesci, B.L. 2006. Palaeomagnetic Analysis of Neotectonic Deformation in the Anatolian accretionary collage, Turkey. In: Dilek, Y. & Pavlides, S. (eds) *Post-Collisional Tectonics and Magmatism in the Eastern Mediterranean Region*. Geological Society of America, Special Papers, **409**, 417–440.
- Piper, J.D.A., Gürsoy, H., Tatar, O., Beck, M.E., Rao, A., Koçbulut, F. & Mesci, B.L. 2010. Distributed neotectonic deformation in the Anatolides of Turkey: a palaeomagnetic analysis. *Tectonophysics*, **488**, 31–50.
- Platzman, E.S., Platt, J.P., Tapırdamaz, C., Sanver, M. & Rundle, C.C. 1994. Why are there no clockwise rotations along the North Anatolian Fault Zone? *Journal of Geophysical Research*, **99**, 21705–21716.
- Platzman, E.S., Tapırdamaz, C. & Sanver, M. 1998. Neogene anticlockwise rotation of central Anatolia (Turkey): Preliminary palaeomagnetic and geochronological results. *Tectonophysics*, **299**, 175–189.
- Purvis, M. & Robertson, A. 2004. A pulsed extension model for the Neogene–Recent E–W-trending Alaşehir Graben and the NE–SW-trending Selendi and Gördes Basins, Western Turkey. *Tectonophysics*, **391**, 171–201.
- Purvis, M. & Robertson, A.H.F. 2005a. Sedimentation of the Neogene–Recent Alaşehir (Gediz) continental graben system used to test alternative tectonic models for western (Aegean) Turkey. *Sedimentary Geology*, **173**, 373–408.
- Purvis, M. & Robertson, A.H.F. 2005b. Miocene sedimentary evolution of the NE–SW-trending Selendi and Gördes Basins, W Turkey: implications for extensional processes. *Sedimentary Geology*, **174**, 31–62.
- Rimmelé, G., Oberhänsli, R., Candan, O., Goffé, B. & Jolivet, L. 2006. The wide distribution of HP–LT rocks in the Lycian Belt, (Western Turkey): implications for accretionary wedge geometry. In: Robertson, A.H.F. & Mountrakis, D. (eds) *Tectonic Development of the Eastern Mediterranean Region*. Geological Society, London, Special Publications, **260**, 447–466, <https://doi.org/10.1144/GSL.SP.2006.260.01.18>
- Ring, U. & Collins, A.S. 2005. U–Pb SIMS dating of synkinematic granites: timing of core-complex formation in the northern Anatolide belt of western Turkey. *Journal of the Geological Society, London*, **162**, 289–298, <https://doi.org/10.1144/0016-764904-016>
- Ring, U., Susanne, L. & Matthias, B. 1999. Structural analysis of a complex nappe sequence and late orogenic basins from the Aegean Island of Samos, Greece. *Journal of Structural Geology*, **21**, 1575–1601.
- Ring, U., Johnson, C., Hetzel, R. & Gessner, K. 2003. Tectonic denudation of a Late Cretaceous–Tertiary collisional belt: Regionally symmetric cooling patterns and their relation to extensional faults in the Anatolide belt of western Turkey. *Geological Magazine*, **140**, 421–441.
- Şan, O. 1998. *Ahmetli (Manisa) güneyinde Menderes masifi ve Tersiyer ortu kayalarının jeolojisi [Geology of the basement and Tertiary cover rocks of Menderes massif in the south of Ahmetli (Manisa)]*. MSc thesis, Ankara University.
- Sarıca, N. 2000. The Plio-Pleistocene age of Büyük Menderes and Gediz Grabens and their tectonic significance on N–S extensional tectonics in West Anatolia: mammalian evidence from the continental deposits. *Geological Journal*, **35**, 1–24.
- Schutt, H. & Besenecker, H. 1973. A mollusc fauna from the Neogene of Chios (Aegean). *Archives Mollusques*, **13**, 1–29.
- Şen, S. & Seyitoğlu, G. 2009. Magnetostratigraphy of early–middle Miocene deposits from east–west trending Alaşehir and Büyük Menderes grabens in western Turkey, and its tectonic implications. In: van Hinsbergen, D.J.J., Edwards, M.A. & Govers, R. (eds) *Collision and Collapse at the Africa–Arabia–Eurasia Subduction Zone*. Geological Society, London, Special Publications, **311**, 321–342, <https://doi.org/10.1144/SP311.13>
- Şengör, A.M.C. 1979. The North Anatolian Transform Fault: its age, offset and tectonic significance. *Journal of the Geological Society, London*, **136**, 269–282, <https://doi.org/10.1144/gsjgs.136.3.0269>
- Şengör, A.M.C. & Yılmaz, Y. 1981. Tethyan evolution of Turkey: a plate tectonic approach. *Tectonophysics*, **75**, 181–241.
- Şengör, A.M.C., Görür, N. & Şaroğlu, F. 1985. Strike-slip faulting and related basin formation in zones of tectonic escape: Turkey as a case study. In: Biddle, K. & Christie-Blick, N. (eds) *Strike-Slip Deformation, Basin Formation and Sedimentation*. Society of Economic Paleontologists and Mineralogists, Special Publication, **37**, 227–264.
- Seyitoğlu, G. & Scott, B.C. 1996. The cause of N–S extensional tectonics in western Turkey: tectonic escape vs back-arc spreading vs orogenic collapse. *Journal of Geodynamics*, **22**, 145–153.
- Seyitoğlu, G., Çemen, İ. & Tekeli, O. 2000. Extensional folding in the Alaşehir (Gediz) Graben, western Turkey. *Journal of the Geological Society, London*, **157**, 1097–1100, <https://doi.org/10.1144/jgs.157.6.1097>
- Seyitoğlu, G., Tekeli, O., Çemen, İ., Şen, Ş. & Işık, V. 2002. The role of the flexural rotation/rolling hinge model in the tectonic evolution of the Alaşehir graben, Western Turkey. *Geological Magazine*, **139**, 15–26.
- Seyitoğlu, G., Işık, V. & Çemen, İ. 2004. Complete Tertiary exhumation history of the Menderes Massif, Western Turkey: an alternative working hypothesis. *Terra Nova*, **16**, 358–363.
- Sözbilir, H. 2001. Extensional tectonics and the geometry of related macroscopic structures: field evidence from the Gediz detachment, western Turkey. *Turkish Journal of Earth Sciences*, **10**, 51–67.
- Sözbilir, H. 2002. Geometry and origin of folding in the Neogene sediments of the Gediz Graben, western Anatolia, Turkey. *Geodinamica Acta*, **15**, 277–288.
- Sözbilir, H. 2005. Oligo-Miocene extension in the Lycian orogen: evidence from the Lycian molasse basin, SW Turkey. *Geodinamica Acta*, **18**, 257–284.
- Sözbilir, H. & Emre, T. 1990. Neogene stratigraphy and structure of the northern rim of the Büyük Menderes graben. In: Savaşçın, M.Y. & Eronat, A.H. (eds) *Proceedings of International Earth Sciences Congress on Aegean Regions*, İzmir, **2**, 314–322.
- Sözbilir, H., İnci, U., Erkul, F. & Sümer, Ö. 2003. An intermittently active transform zone accommodating NS extension in Western Anatolia and its relation to the North Anatolian Fault System. In: Koçyiğit, A. & Eikichi, T. (eds) *International Workshop on the North Anatolian, East Anatolian and Dead Sea Fault Systems: Recent Progress in Tectonics and Paleoseismology*, **87**, Ankara.
- Sözbilir, H., Sarı, B., Uzel, B., Sümer, Ö. & Akkiraz, S. 2011. Tectonic implications of transtensional supradetachment basin development in an extension-parallel transfer zone: the Kocaçay Basin, western Anatolia, Turkey. *Basin Research*, **23**, 423–448.
- Steiger, R.H. & Jäger, E. 1977. Subcommission on geochemistry: convention on the use of decay constants in geo- and cosmochronology. *Earth and Planetary Science Letters*, **36**, 359–362.
- Steininger, F.F. 1999. Chronostratigraphy, geochronology and biochronology of the Miocene European Land Mammal Mega-Zones (ELMMZ) and the Miocene Mammal-Zones. In: Rössner, G. & Heissig, K. (eds) *The Miocene Land Mammals of Europe*. Pfeil, Munich, 9–24.
- Sümer, Ö., İnci, U. & Sözbilir, H. 2012. Tectono-sedimentary evolution of an Early Pleistocene shallow marine fan-deltaic succession at the western coast of Turkey. *Geodinamica Acta*, **25**, 112–131.
- Sümer, Ö., İnci, U. & Sözbilir, H. 2013. Tectonic evolution of the Söke Basin: Extension-dominated transtensional basin formation in western part of the

- Büyük Menderes Graben, Western Anatolia, Turkey. *Journal of Geodynamics*, **65**, 148–175.
- Tatar, O., Piper, J.D.A., Gürsoy, H. & Temiz, H. 1996. Regional significance of neotectonic counterclockwise rotation in Central Turkey. *International Geology Review*, **38**, 692–700.
- Tatar, O., Piper, J.D.A. & Gürsoy, H. 2000. Palaeomagnetic study of the Erciyes sector of the Ecemiş Fault Zone: neotectonic deformation in the southeastern part of the Anatolian Block. In: Bozkurt, E., Winchester, J.A. & Piper, J.D.A. (eds) *Tectonics and Magmatism in Turkey and the Surrounding Area*. Geological Society, London, Special Publications, **173**, 423–440, <https://doi.org/10.1144/GSL.SP.2000.173.01.20>
- Tatar, O., Gürsoy, H. & Piper, J.D.A. 2002. Differential neotectonic rotations in Anatolia and the Tauride Arc: paleomagnetic investigation of the Erenlerdağı Complex and Isparta volcanic district, south–central Turkey. *Journal of the Geological Society, London*, **159**, 283–294, <https://doi.org/10.1144/GSL.SP.1999.159.01.16>
- Tatar, O., Piper, J.D.A., Gürsoy, H., Heimann, A. & Koçbulut, F. 2004. Neotectonic deformation in the transition zone between the Dead Sea Transform and the East Anatolian Fault Zone, Southern Turkey: a palaeomagnetic study of the Karasu Rift Volcanism. *Tectonophysics*, **385**, 17–43.
- Tauxe, L. & Kent, D.V. 2004. A simplified statistical model for the geomagnetic field and the detection of shallow bias in paleomagnetic inclinations: Was the ancient magnetic field dipolar? In: Kelley, D.S., Baross, J.A. & Gary, S.C. (eds) *Timescales of the Paleomagnetic Field*. American Geophysical Union, Geophysical Monograph, **145**, 101–116.
- Tauxe, L. & Watson, G.S. 1994. The fold test: an eigen analysis approach. *Earth and Planetary Science Letters*, **122**, 331–341.
- Tauxe, L., Kodama, K. & Kent, D.V. 2008. Testing corrections for paleomagnetic inclination error in sedimentary rocks: a comparative approach. *Physics of the Earth and Planetary Interiors*, **169**, 152–165.
- Thomson, S.N. & Ring, U. 2006. Thermochronologic evaluation of postcollision extension in the Anatolide orogen, western Turkey. *Tectonics*, **25**, TC3005.
- Tirel, C., Gautier, P., van Hinsbergen, D.J.J. & Wortel, M.J.R. 2009. Sequential development of metamorphic core complexes: numerical simulations and comparison to the Cyclades, Greece. In: van Hinsbergen, D.J.J., Edwards, M. A. & Govers, R. (eds) *Collision and Collapse at the Africa–Arabia–Eurasia Subduction Zone*. Geological Society, London, Special Publications, **311**, 257–292, <https://doi.org/10.1144/SP311.10>
- Ünay, E. & Göktaş, F. 1999. Söke Çevresi (Aydın) Geç-Erken Miyosen ve Kuvaterner yaşlı küçük memelileri: Ön sonuçlar. *Geological Bulletin of Turkey*, **42**, 99–113.
- Ünay, E., Göktaş, F., Hakyemez, H.Y., Avşar, M. & Şan, Ö. 1995. Büyük Menderes Grabeni'nin kuzey kenarındaki çökellerin Arvicolidae (Rodentia, Mammalia) faunasına dayalı olarak yaşlandırılması. *Geological Bulletin of Turkey*, **38**, 75–80.
- Uzel, B. & Sözbilir, H. 2008. A first record of strike-slip basin in western Anatolia and its tectonic implication: The Cumaovası basin as an example. *Turkish Journal of Earth Sciences*, **17**, 559–591.
- Uzel, B., Sözbilir, H., Özkaymak, Ç., Kaymakci, N. & Langereis, C.G. 2013. Structural evidence for strike-slip deformation in the İzmir–Balıkesir transfer zone and consequences for late Cenozoic evolution of western Anatolia (Turkey). *Journal of Geodynamics*, **65**, 94–116.
- Uzel, B., Langereis, C.G., Kaymakci, N., Sözbilir, H., Özkaymak, Ç. & Özkaptan, M. 2015. Paleomagnetic evidence for an inverse rotation history of Western Anatolia during the exhumation of Menderes core complex. *Earth and Planetary Science Letters*, **414**, 108–125.
- van Hinsbergen, D.J.J. & Schmidt, S.M. 2012. Map-view restoration of Aegean–west Anatolian accretion and extension since the Eocene. *Tectonics*, **31**, TC5005.
- van Hinsbergen, D.J.J., Snel, E., Garstman, S.A., Marunteanu, M., Langereis, C., Wortel, M.J.R. & Meulenkaamp, J.E. 2004. Vertical motions in the Aegean volcanic arc: evidence for rapid subsidence preceding volcanic activity on Milos and Aegina. *Marine Geology*, **209**, 329–345.
- van Hinsbergen, D.J.J., Hafkenscheid, E., Spakman, W., Meulenkaamp, J.E. & Wortel, R. 2005a. Nappe stacking resulting from subduction of oceanic and continental lithosphere below Greece. *Geology*, **33**, 325–328.
- van Hinsbergen, D.J.J., Langereis, C.G. & Meulenkaamp, J.E. 2005b. Revision of the timing, magnitude and distribution of Neogene rotations in the western Aegean region. *Tectonophysics*, **396**, 1–34.
- van Hinsbergen, D.J.J., Krijgsman, W., Langereis, C.G., Cornée, J.J., Duemeijer, C.E. & van Vugt, N. 2007. Discrete Plio-Pleistocene phases of tilting and counterclockwise rotation in the southeastern Aegean arc (Rhodos, Greece): early Pliocene formation of the south Aegean left-lateral strike-slip system. *Journal of the Geological Society, London*, **164**, 1133–1144, <https://doi.org/10.1144/0016-76492006-061>
- van Hinsbergen, D.J.J., Dupont-Nivet, G., Nakov, R., Oud, K. & Panaiotu, C. 2008. No significant post-Eocene rotation of the Moesian Platform and Rhodope (Bulgaria): implications for the kinematic evolution of the Carpathian and Aegean arcs. *Earth and Planetary Science Letters*, **273**, 123–156.
- van Hinsbergen, D.J.J., Dekkers, M.J., Bozkurt, E. & Koopman, M. 2010a. Exhumation with a twist: paleomagnetic constraints on the evolution of the Menderes metamorphic core complex, western Turkey. *Tectonics*, **29**, TC3009.
- van Hinsbergen, D.J.J., Kaymakci, N., Spakman, W., Torsvik, T.H. & Amaru, M. 2010b. Reconciling geological history with mantle structure in western Turkey. *Earth and Planetary Science Letters*, **297**, 674–686.
- Walcott, C.R. & White, S.H. 1998. Constraints on the kinematics of post-orogenic extension imposed by stretching lineations in the Aegean region. *Tectonophysics*, **298**, 155–175.
- Wortel, M.J.R. & Spakman, W. 2000. Subduction and slab detachment in the Mediterranean–Carpathian region. *Science*, **290**, 1910–1917.
- Yazman, M.K., Güven, A. *et al.* 1998. *Alaşehir Grabeni'nin ve Alaşehir-1 Prospektinin Değerlendirme Raporu*. TPAO Exploration Group, Technical Report, **142**.
- Yılmaz, Y., Genç, Ş.C. *et al.* 1999. Ege Denizi ve Ege bölgesinin jeolojisi ve evrimi. In: Görür, N. (ed.) *Türkiye Denizleri*. Devlet Planlama Teşkilatı, Türkiye Bilimsel ve Teknolojik Araştırma Kurumu yayını, Ankara, 211–337.
- Yılmaz, Y., Genç, Ş.C. *et al.* 2000. When did the western Anatolian grabens begin to develop? In: Bozkurt, E., Winchester, J.A. & Piper, J.D.A. (eds) *Tectonics and Magmatism in Turkey and the Surrounding Area*. Geological Society, London, Special Publications, **173**, 353–384, <https://doi.org/10.1144/GSL.SP.2000.173.01.17>
- Zijderveld, J.D.A. 1967. A.C. demagnetization of rocks: analysis of results. In: Collinson, D.W., Creer, K.M. & Runcorn, S.K. (eds) *Methods in Palaeomagnetism*. Elsevier, Amsterdam, 254–286.